

## Chapter 3 Seismic Procedures

### 3-1. General Seismic Methods

Seismic methods are the most commonly conducted geophysical surveys for engineering investigations. Most students of geophysics learn the analogies of optical laws to seismic wave propagation. Seismic refraction provides engineers and geologists with the most basic of geologic data via simple procedures with common equipment.

*a. Seismic waves.* Any mechanical vibration sensed by personal perception is initiated from a source and travels to the location where the vibration is noted. The vibration is merely a change in the stress state due to some input disturbance. The vibration emanates in all directions that support displacement. The vibration readily passes from one medium to another, and from solids to liquids or gasses and in reverse. A vacuum cannot support mechanical vibratory waves, while electromagnetic waves transit through a vacuum. The direction of travel is called the ray, ray vector, or raypath. A source produces motion in all directions and the locus of first disturbances will form a spherical shell or wave front in a uniform material. There are two major classes of seismic waves: body waves, which pass through the volume of a material; and, surface waves, that exist only near a boundary.

#### (1) Body waves.

(a) The fastest traveling of all seismic waves is the compressional or pressure or primary wave (P-wave). The particle motion of P-waves is extension (dilation) and compression along the propagating direction. P-waves travel through all media that support seismic waves; air waves or noise in gasses, including the atmosphere, are P-waves. Compressional waves in fluids, e.g. water and air, are commonly referred to as acoustic waves.

(b) The second wave type to reach a point through a body is the secondary or transverse or shear wave (S-wave). S-waves travel slightly slower than P-waves in solids. S-waves have particle motion perpendicular to the propagating direction, like the obvious movement of a rope as a displacement speeds along its length. These transverse waves can only transit material that has shear strength. S-waves do not exist in liquids and gasses, as these media have no shear strength.

(c) S-waves may be produced by a traction source or by conversion of P-waves at boundaries. The dominant particle displacement is vertical for SV-waves traveling in a horizontal plane. Particle displacements are horizontal for SH-waves traveling in the vertical plane. SH-waves are often generated for S-wave refraction evaluations of engineering sites.

(d) Elastic body waves passing through homogeneous, isotropic media have well-defined equations of motion. Most geophysical texts, including Grant and West (1965), include displacement potential and wave equations. Utilizing these equations, computations for the wave speed may be uniquely determined. Field surveys can readily obtain wave velocities,  $V_p$  and  $V_s$ ; velocities are in units of length per time, usually meters/second (m/s). A homogeneous, isotropic medium's engineering properties of Young's or elastic modulus ( $E$ ) and shear modulus ( $G$ ) and either density ( $p_b$ ) OR Poisson's ratio ( $\nu$ ) can be determined, if  $V_p$  and  $V_s$  are known. The units of these measures are: moduli in pressure, usually pascals (Pa); density in mass per volume, grams/cubic meter ( $\text{g/m}^3 = 10^{-6} \text{ mg/m}^3$ ); and,  $\nu$ , dimensionless. Manipulation of equations from Grant and West (1965) yields

$$\nu = [(V_p/V_s)^2 - 2] / \{2[(V_p/V_s)^2 - 1]\} \quad (3-1)$$

$$E = p_b V_p^2 (1 - 2\nu)(1 + \nu) / (1 - \nu) \quad (3-2)$$

$$G = E / [2(1 + \nu)] \quad (3-3)$$

$$p_b = G / V_s^2 \quad (3-4)$$

Note that these are not independent equations. Knowing two velocities uniquely determines only TWO unknowns of  $p_b$ ,  $\nu$ , or  $E$ . Shear modulus is dependent on two other values. Poisson's ratio must be from 0.0 to a value less than 0.5 from Equations 3-1 and 3-2. For units at the surface,  $p_b$  can be determined from samples or for the subsurface from boring samples or downhole logging (see paragraph 7-1k(11)). Estimates may be assumed for  $\nu$  by material type. Usually the possible range of  $p_b$  (also called unit mass) is approximated and  $\nu$  is estimated. Equations 3-1 through 3-4 may be compared to the approximate values with some judgement applied; a similar downhole logging technique is developed in paragraph 7-1k(15)(b). Table 3-1 provides some typical values selected from: Hempen and Hatheway (1992) for  $V_p$ ; Das (1994) for dry  $p_b$  of soils; Blake (1975) for  $p_{b,dry}$  of rock; and Prakash (1981) for  $\nu$ . Other estimates of  $p_b$  are contained in Table 5-1 for gravity methods. Blake (1975)

**Table 3-1**  
**Typical/Representative Field Values of  $V_p$ ,  $p_b$ , and  $v$  for Various Materials**

Material	$V_p$ (m/s)	$p_{b,dry}$ (mg/m <sup>3</sup> )	$v$
Air	330		
Damp loam	300-750		
Dry sand	450-900	1.6-2.0	0.3-0.35
Clay	900-1,800	1.3-1.8	~0.5
Fresh, shallow water	1,430-1,490	1.0	
Saturated, loose sand	1,500		
Basal/ lodgement till	1,700-2,300	2.3	
Rock			0.15-0.25
Weathered igneous and metamorphic rock	450-3,700		
Weathered sedimentary rock	600-3,000		
Shale	800-3,700		
Sandstone	2,200-4,000	1.9-2.7	
Metamorphic rock	2,400-6,000		
Unweathered basalt	2,600-4,300	2.2-3.0	
Dolostone and limestone	4,300-6,700	2.5-3.0	
Unweathered granite	4,800-6,700	2.6-3.1	
Steel	6,000		

offers laboratory values of all these parameters, but field values will vary considerably from the lab estimates.

(2) Surface waves. Two recognized disturbances which exist only at "surfaces" or interfaces are Love and Rayleigh waves. Traveling only at the boundary, these waves attenuate rapidly with distance from the surface. Surface waves travel slower than body waves. Love waves travel along the surfaces of layered media, and are most often faster than Rayleigh waves. Love waves have particle displacement similar to SH-waves. Rayleigh waves exhibit vertical and horizontal displacement in the vertical plane of raypath. A point in the path of a Rayleigh wave moves back, down, forward, and up repetitively in an ellipse like ocean waves.

(a) Rayleigh waves are developed by harmonic oscillators, as steady-state motion is achieved around the oscillator's block foundation. The phase measurement of

the wave allows determination of the wavelengths for differing frequencies of the oscillator. A procedure exists for  $G$  to be computed from these measurements.

(b) Surface waves are produced by surface impacts, explosions and wave form changes at boundaries. Love and Rayleigh waves are also portions of the surface wave train in earthquakes. These surface waves may carry greater energy content than body waves. These wave types arrive last, following the body waves, but can produce larger horizontal displacements in surface structures. Therefore surface waves may cause more damage from earthquake vibrations.

*b. Wave theory.* A seismic disturbance moves away from a source location; the locus of points defining the expanding disturbance is termed the wavefront. At any point on a wavefront, the vibration acts as a new source and causes displacements in surrounding positions. The vector normal to the wavefront is the raypath through that point, and is the direction of propagation.

(1) Upon striking a boundary between differing material properties, wave energy is transmitted, reflected, and converted. The properties of the two media and the angle at which the incident raypath strikes will determine the amount of energy: reflected off the surface, refracted into the adjoining material, lost as heat, and changed to other wave types.

(2) An S-wave in rock approaching a boundary of a lake will have an S-wave reflection, a P-wave reflection, and a likely P-wave refraction into the lake water (depending on the properties and incident angle). Since the rock-water boundary will displace, energy will pass into the lake, but the water cannot support an S-wave. The reflected S-wave departs from the boundary at the same angle normal to the boundary as the arriving S-wave struck.

(3) In the case of a P-wave incident on a boundary between two rock types (of differing elastic properties) there may be little conversion to S-waves. Snell's Law provides the angles of reflection and refraction for both the P- and S-waves. [Zoeppritz's equations provide the energy conversion for the body wave forms.] In the rock on the source side (No. 1), the velocities are  $V_{p1}$  and  $V_{s1}$ ; the second rock material (No. 2) has properties of  $V_{p2}$  and  $V_{s2}$ . Then for the incident P-wave ( $P1i$ ), Snell's Law provides the angles of reflections in rock No. 1 and refraction in rock No. 2 as

$$\begin{aligned} \frac{\sin \alpha_{pli}}{V_{p1i}} &= \frac{\sin \alpha_{pl}}{V_{p1}} = \frac{\sin \alpha_{sl}}{V_{s1}} \\ &= \frac{\sin \alpha_{p2}}{V_{p2}} = \frac{\sin \alpha_{s2}}{V_{s2}} \end{aligned} \quad (3-5)$$

(a) The second and third terms of Equation 3-5 are reflections within material No. 1; the fourth and fifth terms are refractions into medium No. 2. Note that none of the angles can exceed 90 deg, since none of the sine terms can be over 1.0, and  $\alpha_{pli} = \alpha_{p1}$ .

(b) Two important considerations develop from understanding Equation 3-5. First is the concept of critical refraction. If rock No. 1 has a lower velocity than rock No. 2 or  $V_{p1} < V_{p2}$ , then from Equation 3-5  $\sin \alpha_{p2} > \sin \alpha_{pli}$  and the refracted  $\alpha_{p2} > \alpha_{pli}$ , the incident angle. Yet  $\sin \alpha_{p2}$  cannot exceed 1.00. The critical incident angle causes the refraction to occur right along the boundary at 90 deg from the normal to the surface. The critical angle is that particular incident angle such that  $\sin \alpha_{p2} = 1.0$  and  $\alpha_{p2} = 90$  deg, or  $\alpha_{(p1)cr} = \sin^{-1}(V_{p1}/V_{p2})$ . Secondly, any incident angle  $> \alpha_{(p1)cr}$  from the normal will cause total reflection back into the source-side material, since  $\sin \alpha_{p2} \nless 1.0$ . For the latter case, all the P-wave energy will be retained in medium No. 1.

(4) Other wave phenomena occur in the subsurface. Diffractions develop at the end of sharp boundaries. Scattering occurs due to inhomogeneities within the medium. As individual objects shrink in size, their effect on scatter is reduced. Objects with mean dimension smaller than one fourth of the wavelength will have little effect on the wave. Losses of energy or attenuation occur with distance of wave passage. Higher frequency waves lose energy more rapidly than waves of lower frequencies, in general.

(5) The wave travels outward from the source in all directions supporting displacements. Energy dissipation is a function of the distance traveled, as the wave propagates away from the source. At boundaries the disturbance passes into other media. If a wave can pass from a particular point A to another point B, Fermat's principle indicates that the raypath taken is the one taking the minimum amount of time. Stated otherwise, the first arrival between two points occurs on the path of least time. In crossing boundaries of media with different properties, the path will not be the shortest distance (a straight line) due to refractions. The actual raypath will have the shortest travel time. Recall that every point on a wavefront is a

new source; thus, azimuths other than that of the fastest arrival will follow paths to other locations for the ever-expanding wave.

*c. Seismic equipment.* Digital electronics have continued to allow the production of better seismic equipment. Newer equipment is hardier, more productive, and able to store greater amounts of data. The choice of seismograph, sensors called geophones, storage medium, and source of the seismic wave depend on the survey being undertaken. The sophistication of the survey, in part, governs the choice of the equipment and the field crew size necessary to obtain the measurements. Cost rises as more elaborate equipment is used. However, there are efficiencies to be gained in proper choice of source, number of geophone emplacements for each line, crew size, channel capacity of the seismograph, and requirements of the field in terrain type and cultural noise.

#### (1) Sources.

(a) The seismic source may be a hammer repetitively striking an aluminum plate or weighted plank, drop weights of varying sizes, a rifle shot, a harmonic oscillator, waterborne mechanisms, or explosives. The energy disturbance for seismic work is most often called the "shot," an archaic term from petroleum seismic exploration. Reference to the "shot" does not necessarily mean an explosive or rifle source was used. The type of survey dictates some source parameters. Smaller mass, higher frequency sources are preferable. Higher frequencies give shorter wavelengths and more precision in choosing arrivals and estimating depths. Yet sufficient energy needs to be entered to obtain a strong return at the end of the survey line.

(b) The type of source for a particular survey is usually known prior to going into the field. A geophysical contractor normally should be given latitude in selecting or changing the source necessary for the task. The client should not hesitate in placing limits on the contractor's indiscriminate use of some sources. In residential or industrial areas perhaps the maximum explosive charge should be limited. The depth of drilling shot holes for explosives or rifle shots may need to be limited; contractors should be cautious not to exceed requirements of permits, utility easements, and contract agreements.

(2) Geophones. The sensor receiving seismic energy is the geophone (hydrophone in waterborne surveys) or phone. These sensors are either accelerometers or velocity transducers, and convert ground shaking into a voltage response. Typically, the amplification of the ground is

many orders of magnitude, but accomplished on a relative basis. The absolute value of particle acceleration cannot be determined, unless the geophones are calibrated.

(a) Most geophones are vertical, single-axis sensors to receive the incoming wave form from beneath the surface. Some geophones have horizontal-axis response for S-wave or surface wave assessments. Triaxial phones, capable of measuring absolute response, are used in specialized surveys. Geophones are chosen for their frequency band response.

(b) The line, spread, or string of phones may contain one to scores of sensors depending on the type of survey. The individual channel of recording normally will have a single phone. Multiple phones per channel may aid in reducing wind noise or airblast or in amplifying deep reflections.

(c) The type, location and number of phones in the spread is invariably left to the field geophysicists to select, modify and adjust. There is rarely any need for the survey purchaser to be involved with decisions concerning the geophones.

(3) Seismographs.

(a) The equipment that records input geophone voltages in a timed sequence is the seismograph. Current practice uses seismographs that store the channels' signals as digital data in discrete time units. Earlier seismographs would record directly to paper or photographic film. Stacking, inputting, and processing the vast volumes of data and archiving the information for the client virtually require digital seismographs.

(b) The seismograph system may be an elaborate amalgam of equipment to trigger or sense the source, digitize geophone signals, store multichannel data, and provide some level of processing display. Sophisticated seismograph equipment is not normally required for engineering and environmental surveys. One major exception is the equipment for subbottom surveys.

(c) The seismic client will have little to do with selection of the appropriate seismograph. The client should state in the contract an acceptable form of providing the field work data. The submitted field information is usually in an electronic form often with a paper graphic version.

(4) Processing. Data processing of seismic information can be as simple as tabular equations for seismic refraction. Processing is normally the most substantial matter the geophysicists will resolve, except for the interpretation.

(a) The client should not require any particular type of seismic processing. The client normally would be advised to know prior to contracting whether the geophysicists will be using off-the-shelf software or privately developed algorithms. Avoid the use of proprietary processing that is not available to the client.

(b) The processing output and interpretation display is a subject of negotiation. The contract should normally specify the minimum level of performance desired by the client.

### 3-2. Seismic Refraction

*a. Introduction.* In a homogeneous medium a bundle of seismic energy travels in a straight line. Upon striking a boundary (between two media of differing seismic properties) at an angle, the direction of travel is changed as it is in the refraction of light at the surface of a pond. Seismic refraction uses this change of direction to derive subsurface information. The path of the energy is denoted by arrows or rays in Figure 3-1. The method of seismic refraction consists of the recording of the time of arrival of the first impulses from a shot at a set of detectors distributed on the surface. On Figure 3-1, a particular set of raypaths are of interest. Those raypaths go downward to the boundary and are refracted along the boundary and return to the surface to impact the detectors. The first arrivals near the shot will have paths directly from the shot to the detector. If the lower material has a higher velocity ( $V_2 > V_1$  in Figure 3-1), rays traveling along the boundary will be the first to arrive at receivers away from the shot. If the time of arrival is plotted on a time-distance curve such as Figure 3-2, the rate of change of arrival times between detectors is seen to be proportional to  $V_2$ , the velocity of the lower material beyond the point identified as  $X_c$  in Figure 3-2.

*b. Theory.*

(1) "Crossover distance"  $X_c$  is defined from a plot of the first arrivals versus distance (Figure 3-2) as the point where the slope of the arrival time curve changes. For the idealized case shown, the curve representing the direct

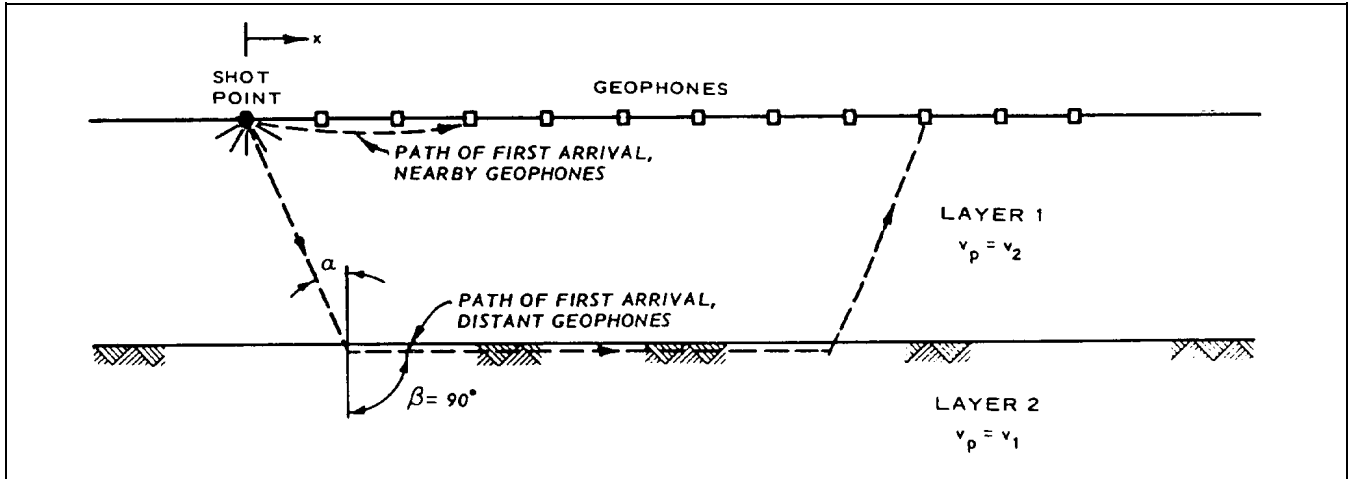


Figure 3-1. Schematic of seismic refraction survey

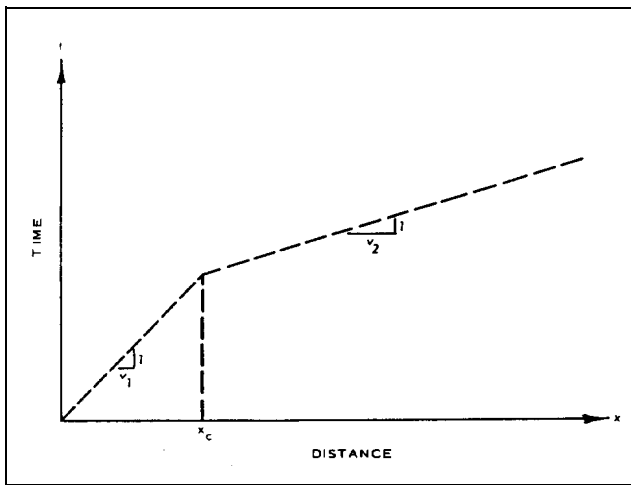


Figure 3-2. Time-versus-distance plot for seismic refraction survey of Figure 3-1

wave is a straight line with a slope equal to the reciprocal of the velocity of the surface layer  $V_1$ . For those raypaths refracted through the second layer, Figure 3-3 demonstrates that the distance traveled in the surface layer is the same for all geophones. Therefore, the travel-time difference from one geophone to the next is the time required for the wave to travel in the lower layer along a horizontal path whose length is the same as the distance between the two geophones. The portion of the curve representing the refracted wave is thus a straight line with a slope equal to the reciprocal of the velocity of the wave in the second layer. The crossover distance is the point where the first arrival is made up of refracted energy.

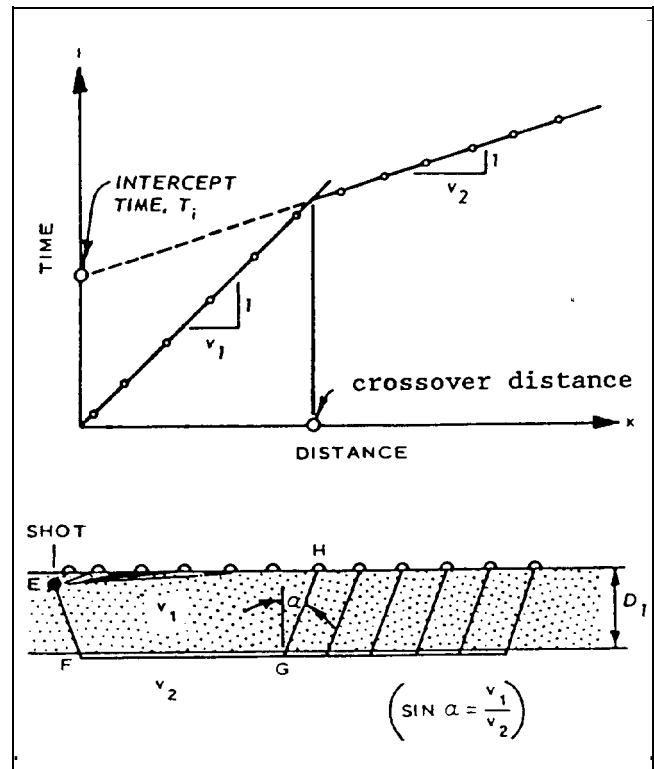


Figure 3-3. Simple two-layer case with plane, parallel boundaries, and corresponding time-distance curve (Redpath 1973)

(2) By consideration of Figure 3-3 two important equations can be identified, one for the intercept time and one for the crossover distance. The expression for travel

time in the refracted layer for the case of the plane layer parallel to the surface is given by

$$T_{sr} = (1/V_2) D_{sr} + 2D_1 (V_2^2 - V_1^2)^{1/2} / (V_1 V_2)$$

where

$T_{sr}$  = time to travel from source to receiver  
(beyond the crossover distance)

$D_{sr}$  = distance from source to receiver

$V_{1 \text{ or } 2}$  = velocity of layer 1 or 2

$D_1$  = depth to first, flat lying interface

By analogy with a straight line whose equation is  $y = mx + b$ , the intercept time is the second term in the above equation:

$$T_i = 2D_1 (V_2^2 - V_1^2)^{1/2} / V_1 V_2$$

or

$$D_1 = (T_i/2) (V_1 V_2) / (V_2^2 - V_1^2)^{1/2} \quad (3-6)$$

where

$T_i$  = intercept time

These equations assume knowledge of  $V_2$  which is easily derived from the travel time curve for this case of flat, plane layers only.  $V_2$  is the inverse of the slope of the travel-time curve beyond the crossover distance (see Figure 3-3). Equation 3-6 can be used for a rudimentary form of interpretation and depth estimation as is discussed below in Section 3-2d.

(3) The other equation of interest is that for the crossover distance:

$$D_1 = (X_c/2) \{ (V_2 - V_1) / (V_2 + V_1) \}^{1/2} \quad (3-7)$$

where

$X_c$  = crossover distance

$D_1$  = depth to a horizontal refracting interface

and the other variables are defined above.

Equation 3-7 is most useful for survey design. Note that information about the lower layer is derived from arrivals beyond the crossover distance. Thus, the length of the refraction line must be longer than the  $X_c$  indicated by this equation.

(4) Figure 3-4 is a plot of velocity ratio ( $V_2/V_1$ ) versus crossover distance to depth ratio ( $X_c/D_1$ ). From that plot, if  $V_1$  is 1,500 m/s and  $V_2$  is 3,000 m/s, the crossover distance will be about 3.4 times the depth. Thus if the boundary under investigation averages 10 m of depth, data about the depth to the second layer would be recorded beyond 35 m (3.4 times 10 m) from the shot. A refraction line longer than 35 m (70 to 100 m is suggested) would be required to investigate the properties of the second layer.

c. *Interpretational methods.* Interpretational methods for refraction can be broadly grouped into the following three classes:

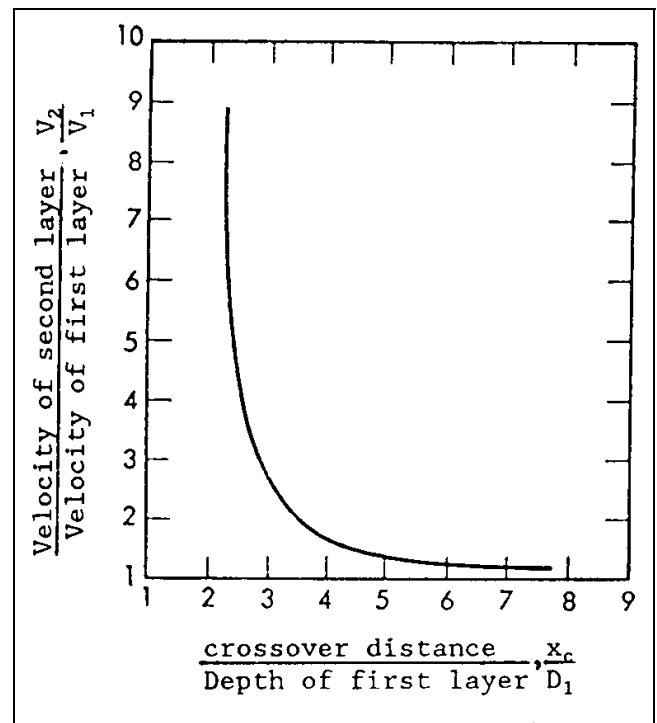


Figure 3-4. Plot of ratio of crossover distance to depth of first layer as a function of velocity contrast (Redpath 1973)

- (1) Intercept-time methods.
- (2) Reciprocal or delay-time methods.
- (3) Ray-tracing.

The level of computation required becomes progressively larger from method to method. Intercept-time methods can be done with pencil and calculator (or at most a spreadsheet computer program). Reciprocal time methods vary from a simple version (given below) to a generalized

version, which taxes most personal computers. Ray-tracing methods, in their most elaborate form, require significant computational resources.

*d. Time-intercept methods.* The basic equation for the time-intercept method is given above in paragraph 3-2b(2). It is interesting to note that Equation 3-7 for the crossover distance can also be solved for depth. This equation can be used to interpret data when, for some reason, the shot initiation time was not recorded (unknown cap delay, etc.).

(1) Single-dipping layer case. Incorporation of dip, as in Figure 3-5, yields several complications:

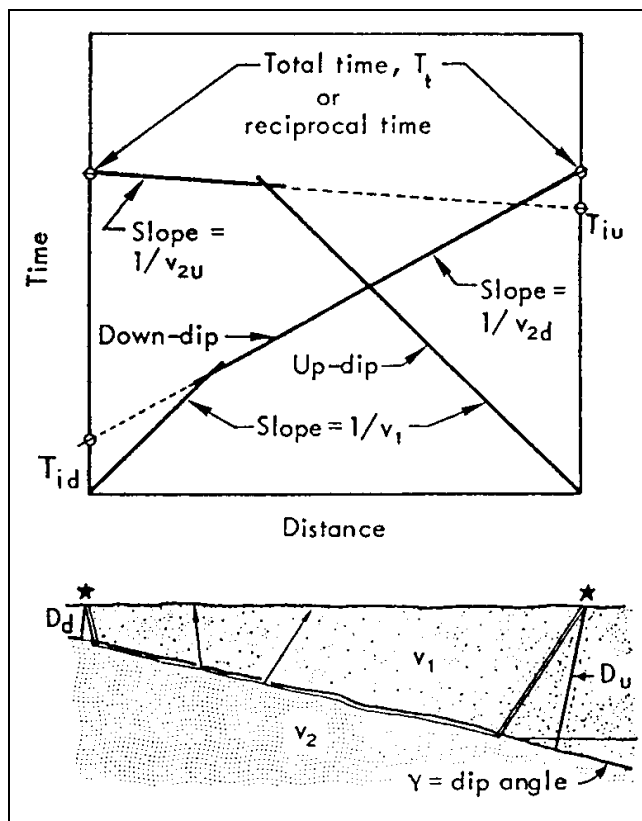


**Figure 3-5. Example of dipping interface and concepts of "reverse shooting" and "apparent velocity" (Redpath 1973)**

(a) Observed velocities of the lower layer are apparent velocities (corresponding to  $V_{2u}$  and  $V_{2d}$  in Figure 3-5) and vary significantly with dip (higher than the true velocity for up-dip, lower for down-dip).

(b) Depths, if determined from intercept times, are slant depths (corresponding to  $D_d$  and  $D_u$  in Figure 3-5) and not depths beneath the shotpoint.

(c) Reversed shots are required, as shots in only one direction measure an apparent velocity ( $V_{2u}$  or  $V_{2d}$ ) for the second layer.

Equations for the slant depths are:

$$\begin{aligned} D_u &= V_1 T_{iu} / (2 \cos \alpha) \\ D_d &= V_1 T_{id} / (2 \cos \alpha) \end{aligned} \quad (3-8)$$

where

$D_u$  = slant depth under the up-dip shot

$D_d$  = slant depth under the down-dip shot

$V_1$  = velocity of the surface material

$T_{iu}$  = up-dip intercept time

$T_{id}$  = down-dip intercept time

$$\cos \alpha = (V_2^2 - V_1^2)^{1/2} / V_2$$

A useful approximation for  $V_2$  (which cannot be measured directly from the travel time curves) is

$$V_2 = (2V_{2u}V_{2d}) / (V_{2u} + V_{2d}) \cos \delta \quad (3-9)$$

where

$V_2$  = approximation to the velocity of the lower medium

$V_{2u}$  = apparent velocity of the lower medium measured up-dip

$V_{2d}$  = apparent velocity of the lower medium measured down-dip

$\delta$  = the approximate angle of dip of the section

An equation for  $\delta$  is

$$\delta = (1/2)(\sin^{-1}(V_1/V_{2d}) - \sin^{-1}(V_1/V_{2u}))$$

Often the cosine of  $\delta$  is approximated as 1.0, thus implying low dips. It should be stressed that the primary assumption in the use of intercept-time methods is that THE LAYER BOUNDARY IS PLANAR. Note that this assumption allows us to use information derived from observations (arrivals) beyond the crossover distance to derive a depth which is assigned to the vicinity of the

shot point. Nevertheless, these methods are useful for a pencil and paper estimate of depths and for a reality check on the more esoteric interpretational techniques.

(2) Multilayer cases. A multilayer case is illustrated in Figure 3-6 for flat-lying layers. Because of the ubiquity of a water layer, most shallow engineering surveys are three-layer cases. The principles of GRM remain the same, with overlap (arrivals from both directions) for all layers necessary. For flat-lying layers, the following time travel equations are useful for modeling purposes. The thickness  $D_1$  of the first layer is found by using the two-layer case and either the intercept time  $T_{i2}$  of the second line segment or the critical distance  $X_{c2}$  determined from the first two line segments. This thickness is used in computing that of the next lower layer  $D_2$  as follows:

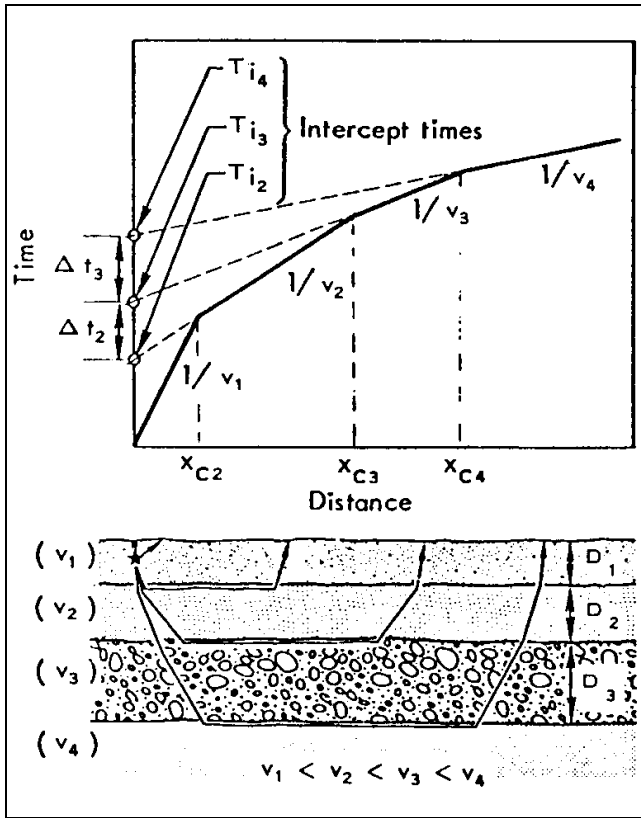


Figure 3-6. Schematic of multiple-layer case and corresponding time-distance curve (Redpath 1973)

$$D_2 = \frac{T_{i3} V_2 V_3}{2\sqrt{V_3^2 - V_2^2}} - D_1 \left( \frac{V_2}{V_1} \right) \sqrt{\frac{V_3^2 - V_1^2}{V_3^2 - V_2^2}} \quad (3-10)$$

where

$V_n$  = velocity of the nth layer

$T_{in}$  = nth intercept time

The equivalent of the above equation, in terms of critical distance, is:

$$D_2 = \frac{X_{c3}}{2} \sqrt{\frac{V_3 - V_2}{V_3 + V_2}} + \frac{D_1}{V_1} \left( \frac{V_3 \sqrt{V_2^2 - V_1^2} - V_2 \sqrt{V_3^2 - V_1^2}}{\sqrt{V_3^2 - V_2^2}} \right) \quad (3-11)$$

where

$D_n$  = depth to the nth refractor

$X_{cn}$  = nth crossover distance

The computations can be extended to deeper layers by use of either of the general equations:

$$D_n = \frac{T_{in-1} V_n V_{n-1}}{2\sqrt{V_{n-1}^2 - V_n^2}} - \sum_{j=1}^{n-1} D_j \left( \frac{V_n}{V_j} \right) \sqrt{\frac{V_{n-1}^2 - V_j^2}{V_{n-1}^2 - V_n^2}} \quad (3-12)$$

and

$$D_n = \frac{X_{cn-1}}{2} \sqrt{\frac{V_{n-1} - V_n}{V_{n-1} + V_n}} + \sum_{j=1}^{n-1} \frac{D_j}{V_j} \left( \frac{V_{n-1} \sqrt{V_n^2 - V_j^2} - V_n \sqrt{V_{n-1}^2 - V_j^2}}{\sqrt{V_{n-1}^2 - V_n^2}} \right) \quad (3-13)$$

Because the equations in this form contain the thicknesses of shallower layers, the computation begins with the first layer and progresses downward. Note that these equations do not incorporate dip. The equations for dipping plane layers are found in Palmer (1980).

*e. Reciprocal methods.* Reciprocal methods include more than 20 methods of interpretation, including those



lumped under the heading of delay-time methods (which may or may not require the measurement of a reciprocal time). The definition of reciprocal time is the travel time along the refractor from one shotpoint to another shotpoint.

(1) Simple reciprocal method. Figure 3-7 illustrates one version of the method. From the figure it can be seen that  $T_{AG} + T_{BG} - T_{AB}$  is equal to the sum of the slant times plus a small time corresponding to travel between the two points where the raypaths emerge from the refractor. For flat-lying, near-plane refractors, these times can be converted to a distance by the equation

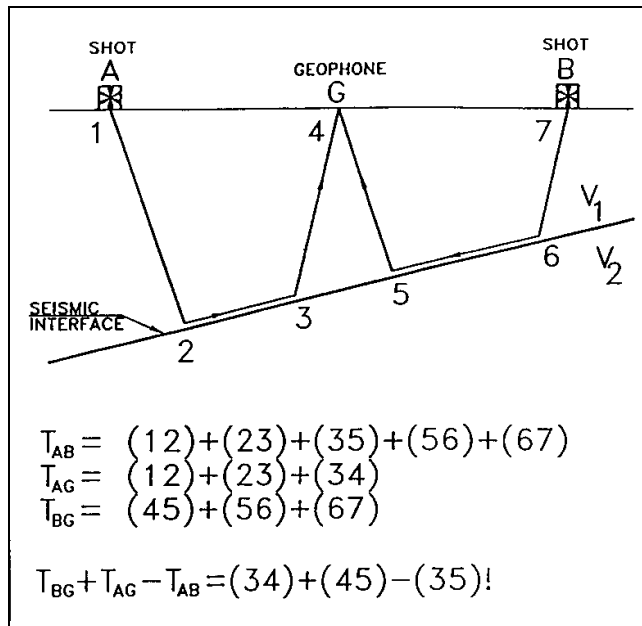


Figure 3-7. Development of simple reciprocal-time method equations

$$Z_G \approx (2V_1 / \cos \alpha)(T_{AB} + T_{BG} - T_{AG})$$

where

$Z_G$  = distance to the refractor from the geophone G

$T_{AB}$  = travel time from shotpoint A to shotpoint B

$T_{AG}$  = travel time from shotpoint A to geophone G

$T_{BG}$  = travel time from shotpoint B to geophone G

$V_1$  = velocity of the upper layer

$\cos \alpha$  is given by  $(V_2^2 - V_1^2)^{1/2} / V_2$

Note that the calculation of  $\cos \alpha$  requires the value of  $V_2$ . As above, a satisfactory approximation is given by Equation 3-9. The angle  $\delta$  is an approximation of the dip for the whole line.

(2) Calculations of depths using this method can easily be completed using a calculator and pencil and paper. Two caveats are in order for this version of reciprocal time methods. One is that "Tab" must be the time on the same refractor from shotpoint to shotpoint. In the presence of deeper refractors, care must be exercised that the reciprocal time is accurate. Secondly, note that the approximations are based on "low" dip. Generally 10-15 deg is an acceptable range.

(3) The distance obtained is measured from the location of the geophone in three dimensions. Thus, there is no requirement for a datum as the distance (depth) is measured from the geophone elevation. Note that the direction is not specified, thus an arc of acceptable points on the refractor is actually defined by this distance. It is instructive to prepare a display of the loci of acceptable solutions for an irregular refractor which is made up of the arcs for all of the geophones along a line (Figure 3-8).

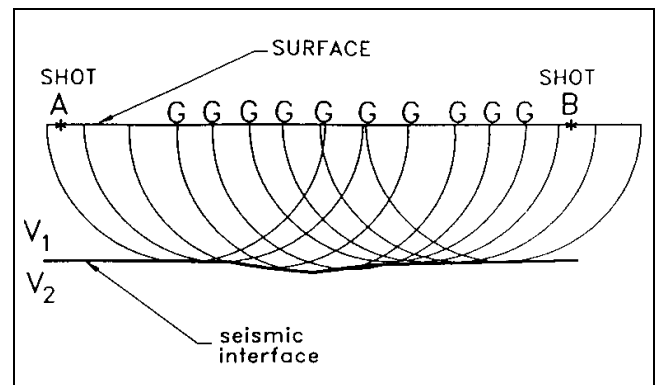


Figure 3-8. Illustration of loci of time depths

(4) Generalized reciprocal method (GRM). Detailed consideration of the above simplified method reveals two major problems when it is applied to extreme topography on the ground surface or subsurface interfaces. First in the determination of  $V_2$ , the above method utilized an average  $V_2$  over a large section of the travel-time curve. Secondly, in the derivation, the segment on the refractor (segment 3-5 in Figure 3-7) was ignored. The generalized reciprocal method or GRM (Palmer 1980) was developed to overcome these and other shortcomings of simpler methods.

(5) Palmer's method derives two functions: the velocity analysis function and the time-depth analysis function. One facet of the method is the use of arrivals at geophone points on either side of the geophone being considered (positions X and Y in Figure 3-9).

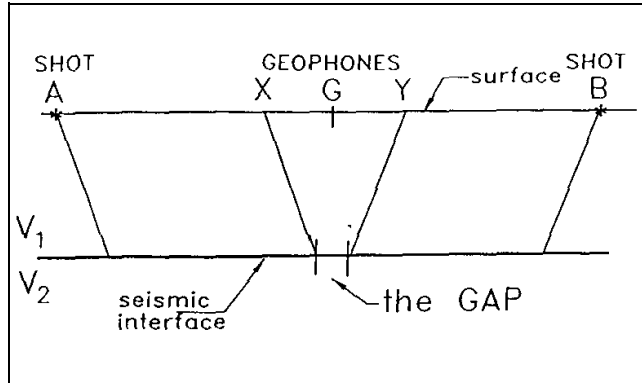


Figure 3-9. Spatial relationships in the GRM methods

(6) Velocity analysis function. Figure 3-10 indicates the derivation of the velocity analysis function. Following the previous nomenclature, this function is formed for  $T_{AB} - T_{AX} - T_{BY}$ . From Figure 3-10, it is seen that this time represents travel time from the shot A to a point on the refractor. If this time is plotted versus geophone position, an accurate  $V_2$ , irrespective of dip or refractor topography can be derived (Figure 3-10). One variable of this arrangement is XY. Figure 3-11 depicts how this factor affects the calculation of  $V_2$ . If XY is chosen so that the exit point on the refractor is common, the travel time, and thus the calculation of  $V_2$ , is dependent only on the material itself. If an incorrect XY such as X'Y' is chosen, structure of arbitrary shape is incorporated in the travel time and thus in the velocity calculation.

(7) Most computer programs performing a GRM prepare an estimate of the travel time given above as a function of XY. Under the assumption that  $V_2$  is constant or slowly varying, inspection of these curves will indicate which XY is correct. The XY showing maximum smoothness (less structure) will conform to the geophysical assumption that is valid for most geology. This part of the process has a twofold purpose, to map  $V_2$  across the spread, and to estimate XY, an important factor to be used in the next section.

(8) Time-depth analysis function. Figure 3-12 indicates the definition of the time-depth analysis function  $T_G$ :

$$T_G = T_{AY} + T_{BX} - T_{AB} - XY/V_2$$

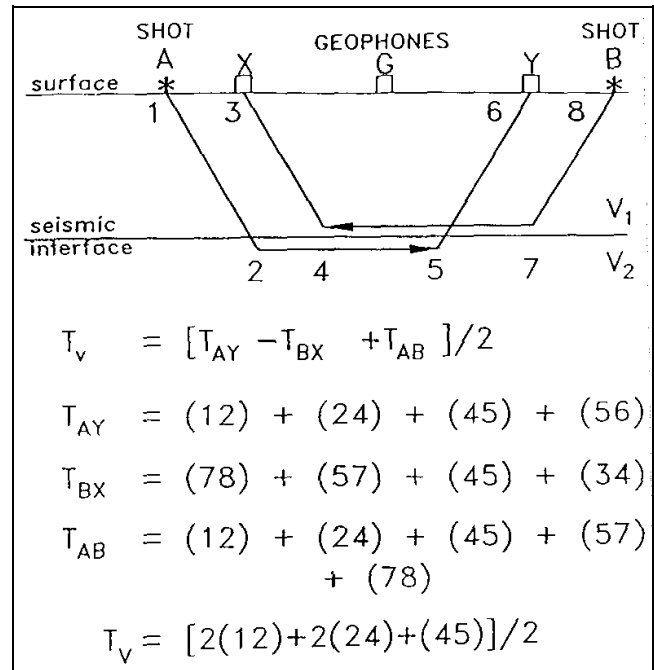


Figure 3-10. Definition of the velocity analysis function

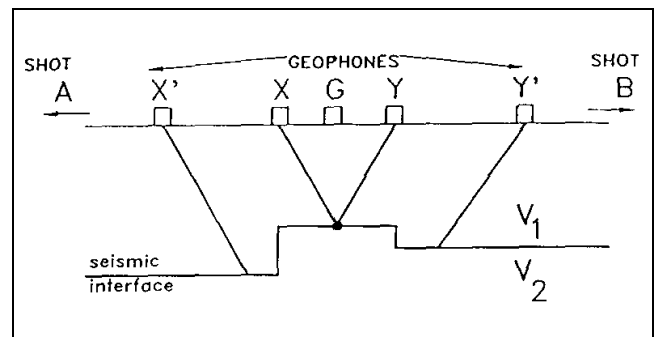


Figure 3-11. Illustration of error in determination of velocity analysis function

where the variables are defined above.

(9) From the analysis in Figure 3-13, it is seen that  $T_G$  represents the two travel times for the slant depths and a correction factor for the distance traveled at  $V_2$  (4-5 in Figure 3-13). This time-depth is analogous to the one developed in the simpler reciprocal method given above but one which can be converted to a depth with a more robust approximation. Before attacking that problem, consider the effects of XY on the calculation of  $T_G$ . Figure 3-14 indicates that if XY is chosen so that the exit points are the same in both directions, the effects of any propagation at  $V_2$  are minimized and the actual structure is mapped. If X'Y' is chosen, a smoothing of consecutive time-depths will occur.

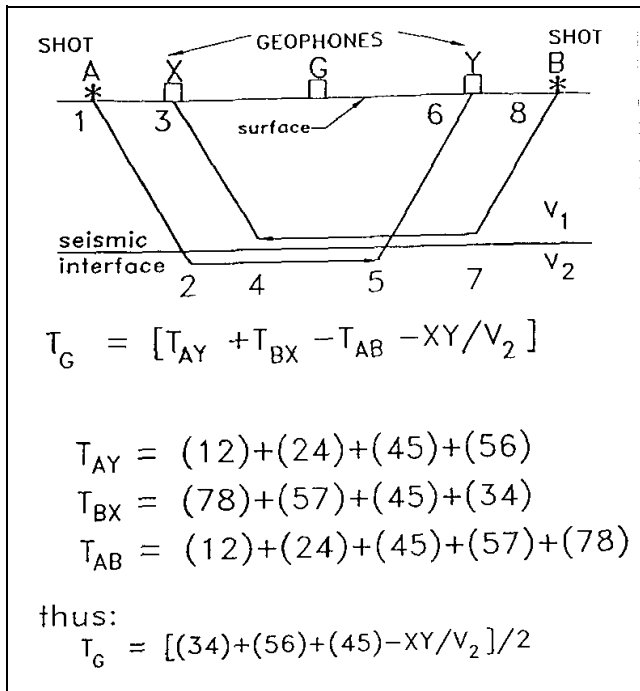


Figure 3-12. Definition of time-depth analysis function

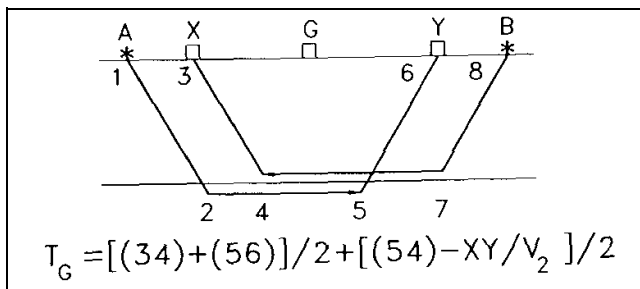


Figure 3-13. Relationships in the time-depth determinations

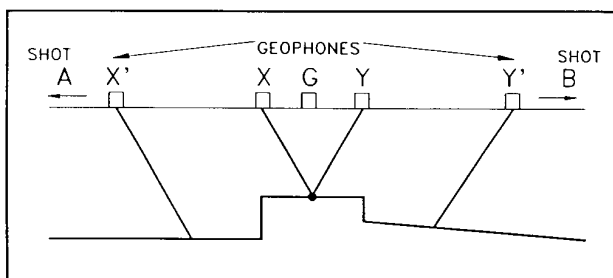


Figure 3-14. Illustration of error in determination of time-depth analysis function

(10) Most computer programs calculate the time depths for several sets of XY's. Under the assumption

that the structure is irregular, the set of time depths with "maximum roughness" is chosen. Thus another estimate of XY is obtained in addition to the one obtained from the velocity analysis function.

(11) Optimum XY. If a model is completely defined; that is, depths and velocities are given, the best XY; that is, the XY with a common exit point on the refractor, can be calculated for flat-lying layers. Figure 3-15 indicates a simple derivation of XY for the flat-lying case. This value of XY, the third in the series, is called the optimum XY. A consistent, complete interpretation will produce a near equal set of XY's. Hidden layers and velocity inversions (both defined later) will manifest themselves as variations in the appropriate XY's.

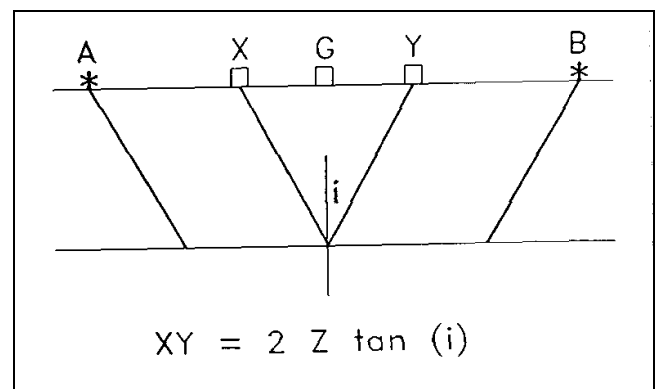


Figure 3-15. Definition of optimum XY

(12) As before, the conversion of time-depths to actual depths requires a velocity corresponding to the slant-distance travel in the upper layer. Palmer gives an acceptable approximation as

$$Z_G = T_G V_1 V_2 / (V_2^2 - V_1^2)^{1/2}$$

which is a sound approximation for low dip angles (up to about 15 deg). As in the previous derivation, this distance is independent of direction and determines only a loci of possible refractor locations (see Figure 3-8).

(13) A full GRM interpretation requires the following data:

(a) An arrival time from the same refractor from both directions at each geophone.

(b) A reciprocal time for energy traveling on that refractor.

(c) A closely spaced set of geophones so that a variety of XY's can be calculated.

(14) These requirements imply a significant increase in the field effort. Geophone spacings of one fourth to one eighth of the depth to the refractor may be required. The number of shots is determined by requirement 1 above, arrival times from both directions on the same refractor. Shot-to-shot distances longer than twice the crossover distance for the first refractor are required. If deeper refractors are present, the shot-to-shot distances must be less than the crossover distance of the deeper refractor. For poorly expressed (almost hidden) and thin layers, the number of shots required may be cost-prohibitive.

*f. Ray-tracing methods.* Ray-tracing programs usually derive some first approximation of a model based on one of the methods described above. A calculation of the expected arrival time at a geophone based on the starting model is then calculated. This calculation becomes quite involved as the complexity of the model increases. As there is no closed form solution for the calculations, iterative methods of generating raypaths are used and convergence must sometimes be forced as the models become more complex.

(1) After the model times have been calculated for the arrivals at the geophones, some form of model adjustment is made which will cause the calculated times to become closer to the observed times. Once the adjustment is made, the process starts over again with calculation of travel times based on the adjusted model. This process is a form of geophysical inversion, i.e., production of a geophysical model which accounts for the observations by calculation of the responses of a model and adjustment of that model. Successful geophysical inversions have several general properties:

(a) The number of observations is generally several times larger than the number of parameters to be determined (that is, the number of shots and observed travel times is far larger than the number of velocities, layers, and inflection points on the layers).

(b) The geophysical model is substantially similar to the geological model being measured (i.e. the approximately flat-lying, low-dip geophysical model is not forced on a geological model of vertical bedding with significant horizontal velocity changes between geophones).

(2) Ray-tracing programs using the appropriate approximations necessary for computation on personal computers are available and are stiff competition for programs based on generalized reciprocal methods.

*g. Models.* A pitfall of the reciprocal time methods is that they do not lend themselves to the generation of a forward model. Calculations based on Equation 3-6 are often sufficient and will be illustrated here.

(1) A geophysical investigation is proposed based on a geological model consisting of:

- (a) An alluvial layer 5 to 8 m thick.
- (b) Basalt bedrock.
- (c) Groundwater 3 to 9 m from the surface.

The problem is to map low spots in the bedrock for siting monitoring wells.

(2) The problem is first converted to a geophysical model.

	Thickness (m)		Velocity (m/s)	
	Min	Max	Min	Max
First layer (alluvium above the water surface)	3	8	450	750
Second layer (water- saturated alluvium)	0	5	1,500	1,700
Third layer (bedrock surface)	--	--	3,000	4,300

(a) The following subtle assumptions are implicit in this geophysical model:

- Alluvium (above the groundwater surface) is fairly dense, thus potentially higher velocities of 450 to 750 m/s are postulated.
- Where saturated (possibly as shallow as 3-m depth), the alluvium will have a velocity near that of water, 1,500 m/s (the second layer may be absent (0-m thickness), when the water surface is beneath the basalt's depth - as shallow as 5-m depth).
- The top of the basalt is not weathered and the basalt is generally homogeneous (thus velocities

between 3,000 and 4,300 m/s are indicated, independent of the groundwater surface level).

Depth and velocity values larger or smaller than those given are tested to define the limits of the investigation program.

(b) Four cases are considered:

- Models 1a and 1b: Dry models (layer 2 absent) with alluvial thicknesses of 3 and 8 m. Variation in the bedrock velocity is accounted. Travel time curves for Model 1 are illustrated in Figure 3-16.
- Models 2a and 2b: Wet (layer 2 present) models with 8 m of alluvium, 5 m of it saturated, and the upper 3 m unsaturated. The bottom layer velocity is held at 3,000 m/s and the surface layer's velocities of 450 and 750 m/s are considered. Travel time curves for Model 2 are found on the bottom of Figure 3-16.

(c) Given these model travel-time curves, the following generalizations can be derived:

- Arrivals from the surface layer are only present within 9 m of the shotpoint (3-m geophone spacings are barely small enough to get enough data on the velocity of the surface layer).
- Only a small portion of the travel-time curve is due to refraction from the water layer (thus geophone spacings of 3 m would probably not be small enough to resolve the layer).

(3) Based on the modeling, the following programs could be proposed:

(a) If the layers are flat, contiguous, no faults are suspected, and any bedrock lows are thought to be broad swales (wavelengths greater than 60 m), then a shooting plan based on time-intercept interpretations is possible. (Because of the narrow window available for both surface and water-layer arrivals, geophone intervals of less than 3 m are recommended. As data will be obtained at each shotpoint, shotpoint spacing and line spacing are functions of the data density required. A typical setup might be 2.5-m or smaller geophone spacings, 24-channel recording and shots at both ends and in the middle of each spread of 24 receivers. Note that reversed shots are required (dip is expected) and that arrivals from the water layers may be present on only some of the travel-time curves (see next section on blind layers).

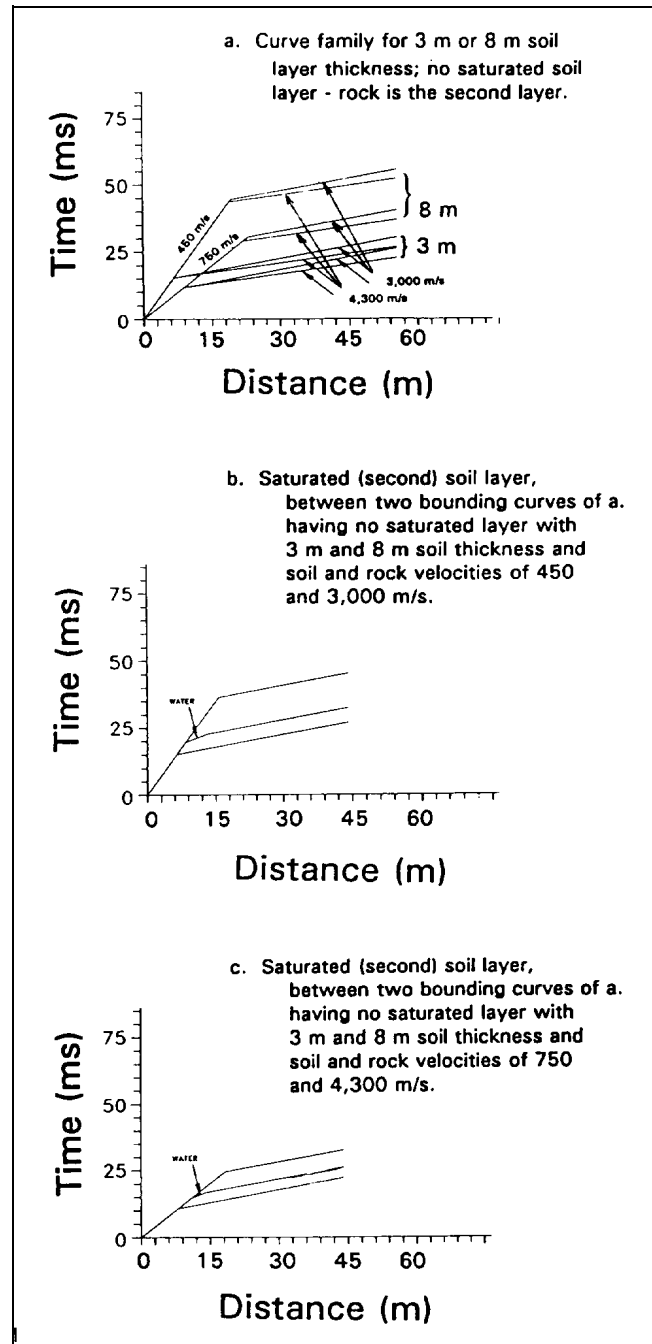


**Figure 3-16. Models of travel-time curves. Time in ms; distance in units of ft (0.3 m = 1.0 ft)**

(b) If the geologic model includes channels cut into the basalt and if the surface of the basalt can exhibit significant structure (say 2- to 3-m elevation changes of channel banks), then a full GRM approach should be taken. The GRM approach to this problem includes the following:

- Geophone spacings of 1.5 m are chosen (to generate a representative set of  $XY$  values, a small interval is necessary).
- One pair of shotpoints offset from the ends of the spread by at least 25 m (thus each geophone will have an arrival from both directions from the high-velocity layer).
- Several sets of shotpoints about 20 m apart. Water arrivals are not present over a very wide range of distances (7 to 12 m in the best case in the models). Thus, shot pairs at these spacings will have to be repeated at least three or four times per spread to get adequate data about the water-bearing layer (see paragraph 3-2i(2)(a) on blind layers).

Thus, a minimum of 10 source locations into a 24-channel spread of 35-m length will be required to generate data adequate for a GRM interpretation. Note that a careful monitoring of the field data is required as the velocities and depths are not usually constant across basaltic terrain.

*h. Field work.* For routine engineering-scale surveys, two to four persons are engaged on a seismic refraction crew. A crew of two will be considerably slower than a crew of three; a crew of four marginally faster than a crew of three unless extensive shothole preparation is necessary. Several fine points of field work to be considered are:

(1) In addition to surveying of the relative locations of shotpoints and geophones to a few percent of the geophone interval, the absolute location of the line should be tied to permanent fiducials at several points. How much error is significant depends on the scale of the problem and the velocities involved. One millisecond (ms) represents 60 cm of travel at 600 m/s, but 3 m at 3,000 m/s. A 30-cm survey error similarly contributes 1/2 to 1/10 ms of time error. The scale of the problem is important. Where closely spaced geophones (3 m or less) and high-frequency signals are used, a 30-cm error is not acceptable. For crustal-scale problems, 30-cm survey error is insignificant.

(2) Electrical noise, usually 60 Hz (cycles per second) in the United States, may be dealt with by the use of internal filters in the seismograph. All filters, analog or digital, cause some time delay of the seismic impulse. Thus, filters should not be adjusted in the course of a survey except in the most unusual circumstance. If not

adjusted, the filter delay becomes part of the accuracy problem, not a precision problem.

(3) Source strength can be adjusted by a variety of techniques; more explosives should be the last technique implemented. Improved coupling for hammer plates or shots (usually by digging a shallow hole), selection of an alternate shot point, more hammer blows, bigger hammers, and other techniques which will occur to the resourceful geophysicist should be tried first. Note that the theoretical variance of random noise due to an increased number of hammer blows decreases as the square root of the number of blows. Thus, unless the shotpoint is particularly important or the cost of physical labor negligible, a practical maximum number of blows is between 10 and 25.

(4) Wet weather causes productivity problems for equipment and personnel. Most geophone-to-cable connections are not waterproof and it is easy to develop a geophone-to-geophone ground loop. The direct impact of raindrops on geophones is easily recorded.

(5) Frozen ground can contribute a high-speed, near-surface path which will obscure the contribution of deeper layers. The P-wave velocity of ice is near 3,800 m/s.

(6) Wind effects can be minimized by putting geophone cables flat down on the ground, anchoring geophone wires, and removing measuring tapes, which flutter in the wind. Geophone burial is a labor-intensive but moderately effective method of dealing with the wind if the wind is not coupled to the ground by nearby vegetation. Sometimes filters will assist in the removal of high-frequency wind or water noise, but paragraph 3-2h(2) above should be considered when using filters.

(7) While human errors cannot be eliminated, the consequences of carelessly placed geophones, improperly recorded locations, and generally sloppy work should be impressed on the entire field crew so that the results produced will be meaningful.

(8) The acoustic wave transmitted through the air may be the first arrival in cases where very low-velocity alluvium is present. In shear-wave work, velocities are often below the velocity of sound in air (345 m/s at standard conditions). Geophone burial and recognition of the acoustic wave when picking the records are mitigation for this source of noise. The air arrival will often cause a first-break of opposite polarity to that caused by transmission through earth materials.

i. Interpretation.

(1) Evaluation of programs. While the geophysical capabilities of commercially available interpretation programs are an obviously important part of any buying decision, the ease of use and applicability of the so-called “front-end” and “back-end” of the program should be carefully considered. Specifically:

(a) Refraction field efforts, even of moderate size, generate enormous amounts of data.

(b) Post-analysis output may be the most important part of the project.

It is imperative to minimize the manual handling of the data. The geometry is entered in the seismograph in the field, a picking program is used to find the first breaks, and these data streams converge in the analysis program. Convenient editing and correction facilities, graphical displays to confirm the correctness of the data entry, and seamless integration are important. A wide variety of printers and plotters for post-analyses should be supported, including the generic digital graphics interchange formats. No matter how good the plate output of the program looks in demonstration, eventually the user will have to do CAD work to get information in the desired form.

(2) Pitfalls. The two most difficult geologic conditions for accurate refraction work are the existence of a thin water-saturated zone just above the bedrock and the existence of a weathered zone at the top of bedrock. These two difficult problems are members of the class of blind zone and hidden layer problems.

(a) Blind zone. The model of paragraph 3-2g is redrawn in Figure 3-17 to emphasize the area immediately above the refractor (shaded). This area is known as the blind zone. Calculation reveals that depending on thickness and velocity, no information (arrivals) will be received from this shaded layer. For velocities lower than  $V_1$ , clearly no refraction will occur. For velocities greater than  $V_1$  but less than  $V_2$ , the travel time curves for a thin zone are shown in Figure 3-18. As thickness or velocity increases, the solid line in Figure 3-18 occurs at earlier times until first arrival information (however sparse) is received from the shaded area. All refractors have a blind zone whose size depends on the depth and velocity distribution.

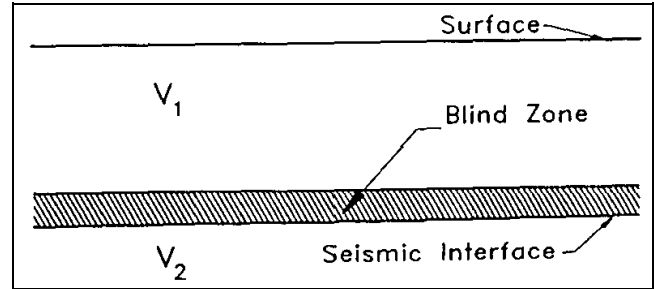


Figure 3-17. Illustration of locating blind zones

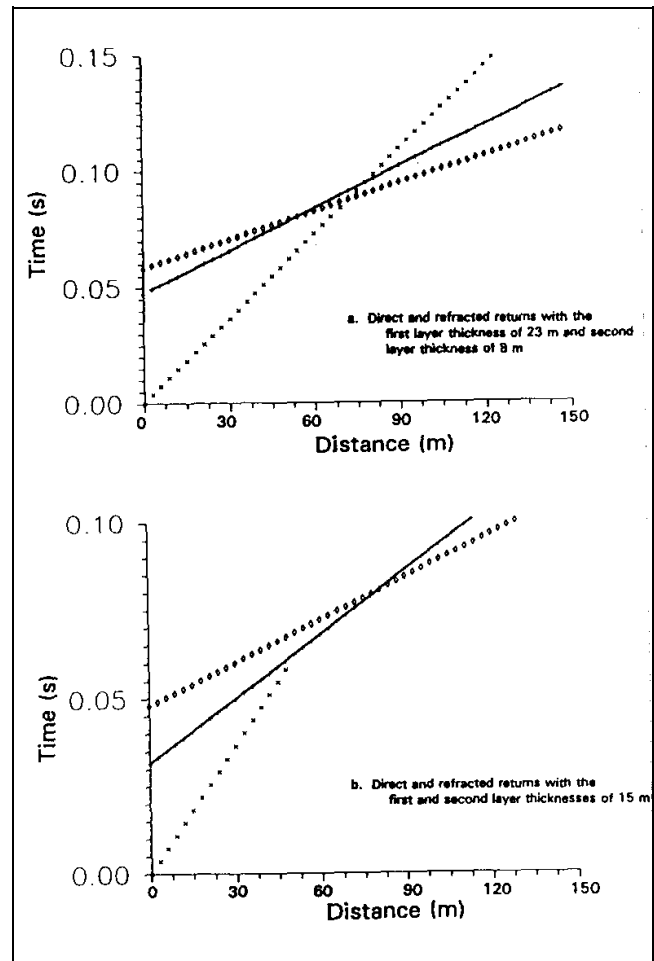


Figure 3-18. Travel-time curves for the hidden-zone problem (0.3 m = 1.0 ft)

(b) Hidden layer. Within all blind zones, there may be a hidden layer of water or weathered bedrock which cannot be detected by the refraction work. Obviously, if the velocity in the blind zone is equal to  $V_1$ , there is no

problem and the interpretation proceeds without error. Other hidden layer issues are the following:

- Water is particularly troublesome, because it often increases the velocity of poorly indurated alluvium to an intermediate velocity between that of unsaturated alluvium (usually 300 to 900 m/s) and bedrock (usually above 2,000 m/s). (The acoustic velocity for water at standard conditions is about 1,500 m/s.)
- Weathered bedrock can act similar to saturated soil. The potential for very rapid lateral changes in the thickness of the weathered layer makes refraction work in saprolitic and similar terrains a difficult proposition. Careful planning and added drilling work could be required.

(c) Two-dimensional assumption. The assumption in the interpretation methods discussed above is that the problem is two-dimensional, i.e., there is no variation of the rock properties or geometry perpendicular to the line. However, the dips measured along lines are apparent dips and a correction is needed to recover true dip.

(d) Inhomogeneity. Some materials, especially glacial deposits or thick man-made layers of uncompacted sediments, will exhibit a continuous increase in velocity with depth. Travel-time curves with a continuous curve or change of slope are an indicator of this situation. Where an approximation of this type of travel-time curve by straight line segments is unsatisfactory, methodology does exist to derive velocity functions of the form of a linear increase with depth or with two-way travel time from the curved travel-time curves (Duska 1963; Hollister 1967).

(3) Case examples. Several common geologic situations which can produce confusing travel-time curves are illustrated in Figures 3-19 to 3-23. Note that other, perhaps less geologically plausible, models could be derived to fit the travel-time curves shown.

(a) Figure 3-19 indicates a simple change in dip. Note that three velocities are recorded, but only two materials are present. Figure 3-20 represents one-half of a buried stream channel and, perhaps in the context of Figure 3-19, is not hard to understand. However, note that four velocities are present. Because the opposite bank of the stream may be present, perhaps on the same spread, the picture can get very complicated.

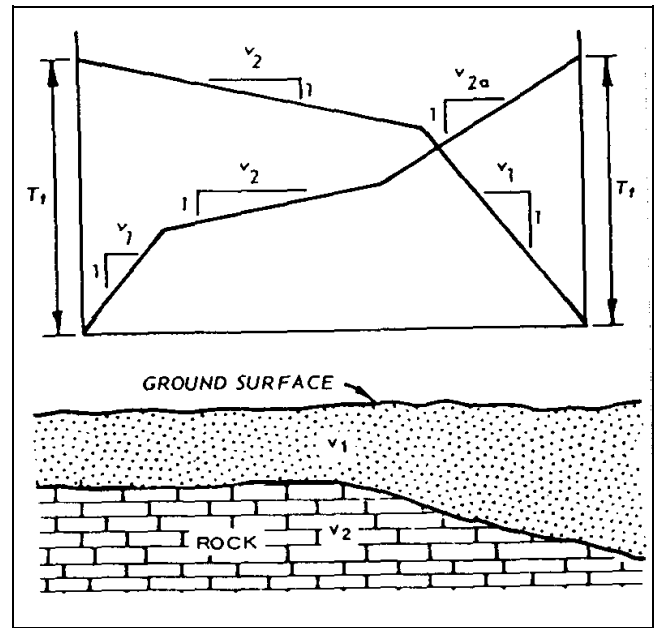


Figure 3-19. Change in dip of refractor surface

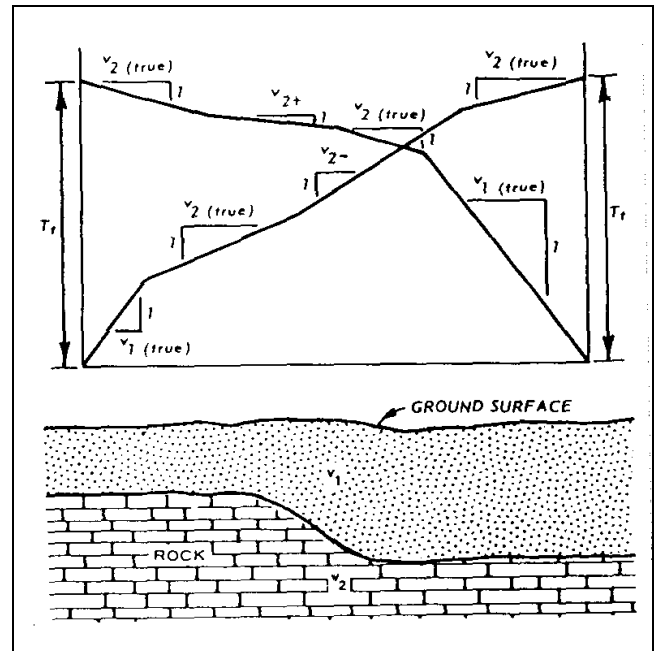


Figure 3-20. Subsurface stream channel

(b) Figures 3-21 and 3-22 indicate another set of models for travel-time curves. Figure 3-22 models a discontinuity in the rock surface and the resultant travel-time curves. Note that the discontinuity causes a delay in both directions while the fault both advances and delays



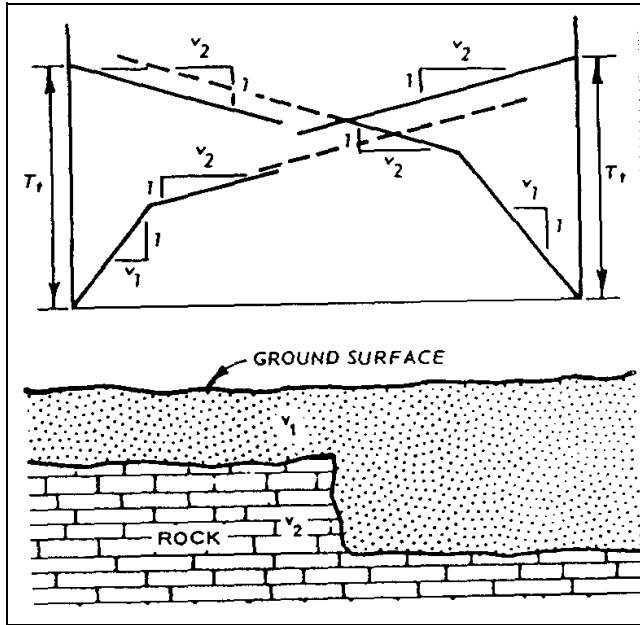


Figure 3-21. Subsurface cliff

the trend of the travel-time curves. One warning about the attempted detection of voids or discontinuities is in order. Fermat's principle says that the discontinuity must extend significantly perpendicular to the profile in order that no fast path detour is present that will minimize the observed delays.

(c) Figure 3-23 is a common setup where a single spread spans a channel. Three velocities are recorded (two of them apparent), if shots are fired only at the ends. When doing cross-channel work, a center shot is usually required to derive the true velocities and geometry from the data recorded.

g. *Shear waves.*

(1) Shear wave (S-wave) measurements have several advantages in engineering and environmental work.

(a) The engineer can relate S-wave velocities more easily to shear moduli and other properties used in engineering calculations. If both compressional (P-wave) and S-wave velocities are measured, Poisson's ratio and other engineering constants can be derived.

(b) In saturated, unconsolidated materials, P-wave velocities are often controlled by water velocity. As S-wave propagation is generally unaffected by the presence of a liquid, S-wave studies are not complicated by

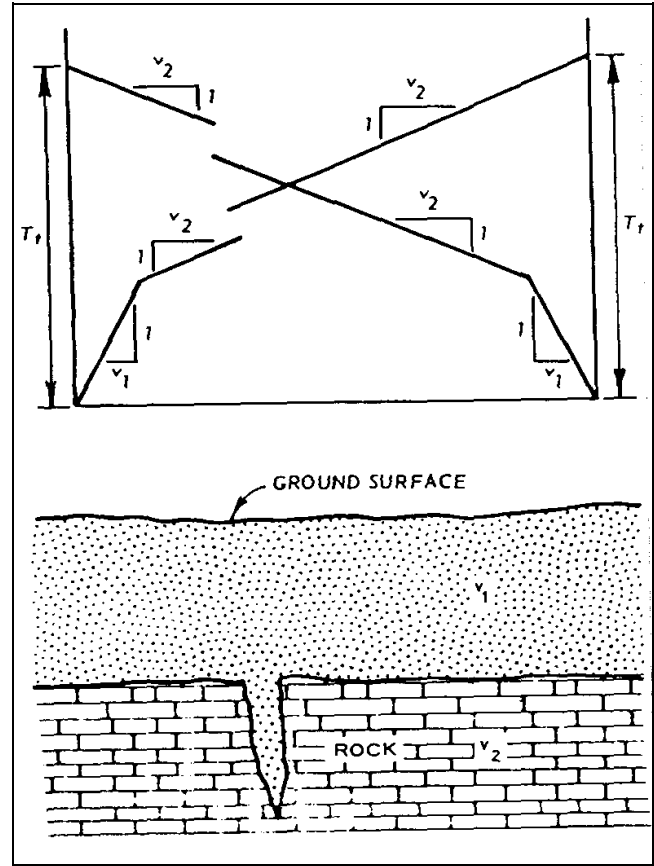


Figure 3-22. Offset in time-distance plot due to discontinuity in rock surface

the location of the water surface. A difficult three-layer P-wave case can become a routine two-layer S-wave case.

(c) As the S-wave measurement by its nature includes a large volume of in situ material, the bulk velocity measurement may be more relevant to the performance of engineered materials than point samples.

(d) S-wave studies are interpreted in the same way as P-wave studies. Differences consist mostly of field technique and some data display methods which will be discussed below.

(2) S-Wave Field Work and Data Recording. S-wave sources have one advantage and one disadvantage which merit discussion. In general, S-wave sources are not as energetic as P-wave sources-there is no "more explosives" alternative to turn to in S-wave work. While large mechanical contraptions have been designed to impart an impressive traction to the ground, their signal strength and reliability remain suspect. The advantage

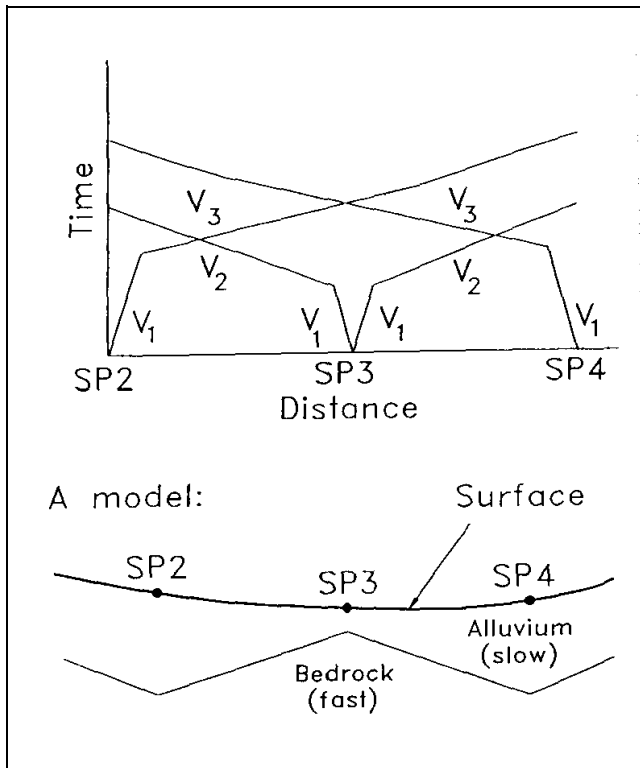


**Figure 3-23. Cross-channel travel-time schematic**

that S-wave sources have is that they have two polarities, both of which can be stacked together to produce record enhancement.

(3) SH-waves, the waves that have particle motion perpendicular to the line of geophones (see Figure 3-24), are preferred for shallow refraction work. This choice minimizes the conversion of S-waves to P-waves at any interface encountered. Thus, a source which produces a traction perpendicular to the line and parallel to the surface is specified (see Figure 3-24). A truck-weighted plank struck on the end with a hammer is the classical source. Portable versions of this type of source and other energetic mechanical sources are available.

(a) Receivers with their sensitive axis oriented perpendicular to the line are also used. Horizontal axis geophones are required, and leveling of each geophone is generally necessary. The geophone axis should be carefully aligned perpendicular to the line and with common polarity (direction).

(b) To utilize the switchable polarity of the source, one field technique is as follows:

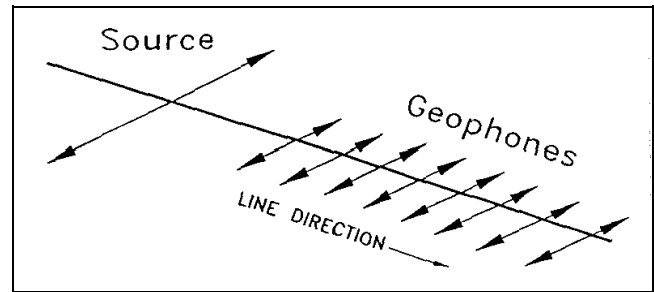


**Figure 3-24. Source and geophone directions for SH waves**

- Shoot (hit) the source in the direction of the polarity of the geophones (stack enough hits to produce reasonable first-breaks with an apparent velocity expected for the known geology of the area. Pitfalls in this stage are the prominent air-blast (345 m/s) and a P-wave water refraction (about 1,600 m/s). Neither of these is the target but either may be the most prominent portion of the record. This first shot is recorded (saved to disk on most modern seismographs) and is called the positive-source-positive-spread record).
- Without erasing the seismograph's contents, move to the other side of the source (this move changes the polarity of the source. Also change the recording polarity of the spread (in most seismographs, this change is accomplished by turning a convenient software switch). To the extent possible, the number of hits and source signature are repeated with the reversed polarity source stacking the data onto the positive-positive record. Save this record as the "stacked" record).
- Clear the seismograph and record the same record (negative source only) as in the previous step. (This record is called the negative-source negative-spread record and is also saved.)

Thus, three records are recorded for each shotpoint. The stacked records enhance the S-wave information and suppress the P-wave information. This suppression takes place because the reversal of the polarity of the source and receivers amplifies the S-wave, but any P-wave energy which has constant polarity is subtracted due to the polarity change. This procedure is illustrated in Figure 3-25.

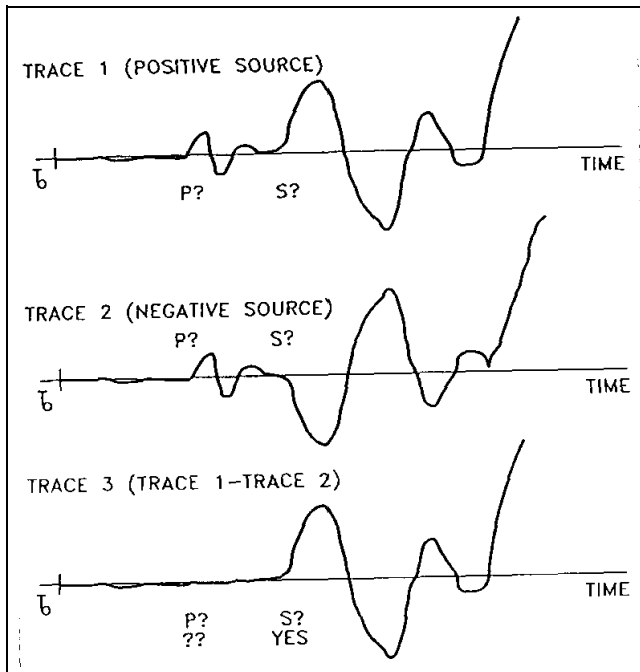


**Figure 3-25. Multiple S-wave recordings**

(c) If the stacked record is of good quality, only cursory examination of the other two records is necessary. However, it is often necessary to use the other records to positively identify the S-wave arrivals if P-wave interference is present. A dual-trace presentation is used to confirm the S-wave arrival.

(4) A sample dual-trace presentation is shown in Figure 3-26. The negative-negative record has been plotted with reversed (again) polarity. Thus any P-wave energy should cause the two traces to move together but any S-wave energy should cause the two traces to diverge. Where the two traces diverge, positive confirmation of S-wave energy is attained. Each shot record may have to be played out in this format to attain positive identification of the S-wave energy.

(5) Additional Considerations. Two fine points of S-wave work are:

(a) Considerable noise suppression of the air-blast and other converted waves can be realized by covering the geophones with some dirt.

(b) Efforts to couple the traction plank or other device to the ground are worthwhile. In soft farmland, the coupling is generally good, but on a rutted gravel road the amount of S-wave energy generated may be small without some shovel work.

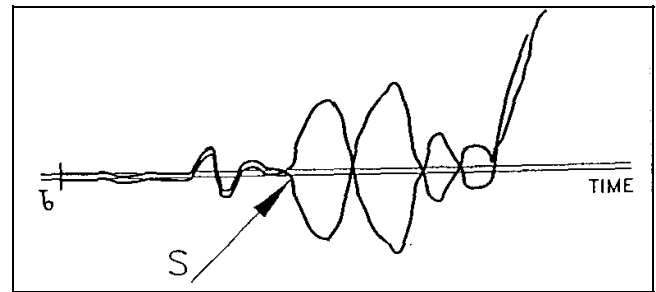


**Figure 3-26. Dual-trace display**

(6) Shear-wave example. A common record in S-wave studies is indicated in Figure 3-27. Arrivals as picked are plotted and the velocity of sound in air is shown for reference. Obviously, sound is going to be a problem at two points on the record.

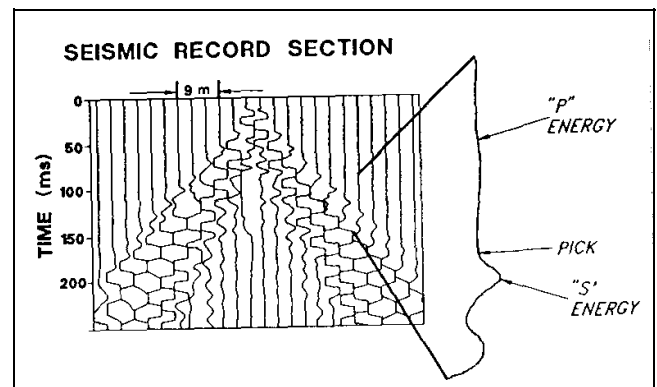


**Figure 3-27. Example of shear-wave record. Expanded trace identifies "S" and "P" energy confirmed by dual trace plots**

### 3-3. Shallow Seismic Reflection

A portion of the seismic energy striking an interface between two differing materials will be reflected from the interface. The ratio of the reflected energy to incident energy is called the reflection coefficient. The reflection coefficient is defined in terms of the densities and seismic velocities of the two materials as:

$$R = (p_{b2}V_2 - p_{b1}V_1)/(p_{b2}V_2 + p_{b1}V_1) \quad (3-14)$$

where

$R$  = reflection coefficient

$p_{b1}, p_{b2}$  = densities of the first and second layers, respectively

$V_1, V_2$  = seismic velocities of the first and second layers, respectively

Modern reflection methods can ordinarily detect isolated interfaces whose reflection coefficients are as small as  $\pm 0.02$ .

*a. Reflection principles.*

(1) The physical process of reflection is illustrated in Figure 3-28, where the raypaths from the successive layers are shown. As in Figure 3-28, there are commonly several layers beneath the earth's surface which contribute reflections to a single seismogram. Thus, seismic reflection data are more complex than refraction data because it is these later arrivals that yield information about the deeper layers. At later times in the record, more noise is present thus making the reflections difficult to extract from the unprocessed record.

(2) Figure 3-29 indicates the paths of arrivals that would be recorded on a multichannel seismograph. Note that Figure 3-29 indicates that the subsurface coverage is exactly one half of the surface distance across the geophone spread. The subsurface sampling interval is one half of the distance between geophones on the surface.

(3) Another important feature of modern reflection-data acquisition is illustrated by Figure 3-30. If multiple shots, S1 and S2, are recorded by multiple receivers, R1 and R2, and the geometry is as shown in the figure, the reflector point for both rays is the same. However, the raypaths are not the same length, thus the reflection will occur at different times on the two traces. This time delay, whose magnitude is indicative of the subsurface velocities, is called normal-moveout. With an appropriate time shift, called the normal-moveout correction, the two traces (S1 to R2 and S2 to R1) can be summed, greatly enhancing the reflected energy and canceling spurious noise.

(a) This method is called the common reflection point, common midpoint, or common depth point (CDP) method. If all receiver locations are used as shot points, the multiplicity of data on one subsurface point (called CDP fold) is equal to one half of the number of recording channels. Thus, a 24-channel seismograph will record 12-fold data if a shot corresponding to every receiver position is shot into a full spread. Thus, for 12-fold data every subsurface point will have 12 separate traces added, after appropriate time shifting, to represent that point.

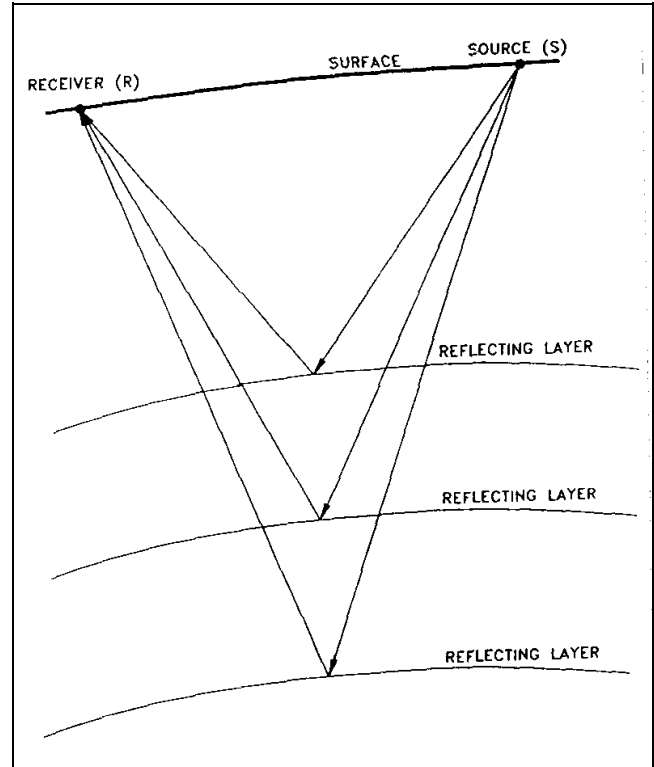


Figure 3-28. Schematic of seismic reflection method

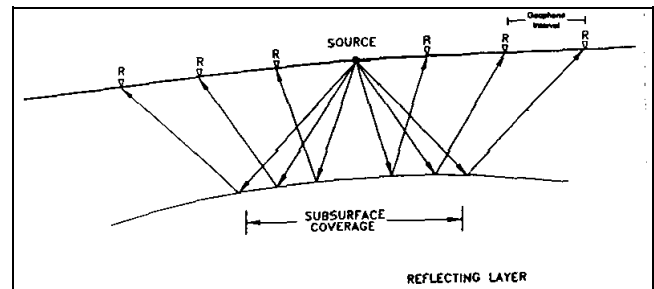


Figure 3-29. Multi-channel recordings for seismic reflection

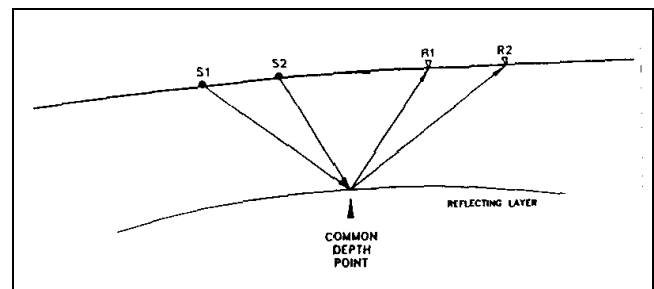
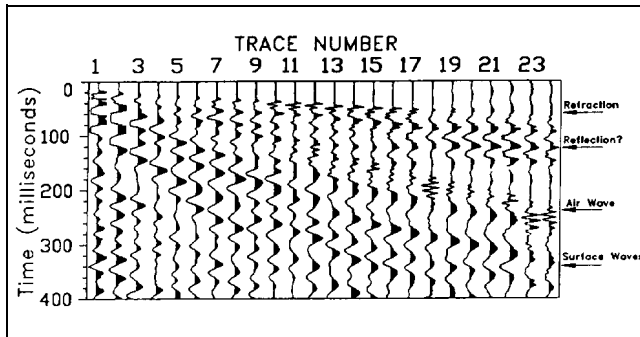


Figure 3-30. Illustration of common-depth point recording

(b) Arrivals on a seismic reflection record can be seen in Figure 3-31. The receivers are arranged to one side of a shot which is 15 m from the first geophone. Various arrivals are identified on Figure 3-31. Note that the gain is increased down the trace to maintain the signals at about the same size by a process known as automatic gain control (AGC). One side of the traces is shaded to enhance the continuity between traces.



**Figure 3-31. Sample seismic reflection record**

(4) The ultimate product of a seismic reflection job is a corrected cross section with reflection events in their true subsurface positions. Though more than 60 years of development have gone into the seismic reflection method in the search for petroleum, the use of reflection for the shallow subsurface (less than 50 m) remains an art. This manual cannot give every detail of the acquisition and processing of shallow seismic reflection data. Thus the difference between deep petroleum-oriented reflection and shallow reflection work suitable for engineering and environmental applications will be stressed.

(5) Cost and frequency bandwidth are the principal differences between the two applications of seismic reflection. One measure of the nominal frequency content of a pulse is the inverse of the time between successive peaks. In the shallow subsurface the exploration objectives are often at depths of 15 to 45 m. At 450 m/s, a wave with 10 ms peak to peak (nominal frequency of 100 Hz) is 45 m long. To detect (much less differentiate between) shallow, closely spaced layers, pulses with nominal frequencies at or above 200 Hz may be required. A value of 1,500 m/s is used as a representative velocity corresponding to saturated, unconsolidated materials because without saturated sediments, both attenuation and lateral variability make reflection generally difficult.

*b. Common offset reflection methods.* A technique for obtaining onefold reflection data is called the common-offset method or common-offset gather (COG). It is

instructive to review the method, but it has fallen into disuse because of the decreased cost of CDP surveys and the difficulty of quantitative interpretation in most cases.

(1) Figure 3-32 illustrates time-distance curves for the seismic waves which can be recorded. In the optimum offset distance range, the reflected and refracted arrivals will be isolated in time. Note that no quantitative scales are shown as the distances, velocities, and wave modes are distinct at each site. Thus testing is necessary to establish the existence and location of the optimum offset window.

(2) Figure 3-33 illustrates the COG method. After the optimum offset distance is selected, the source and receiver are moved across the surface. Note that the subsurface coverage is one-fold and there is no provision for noise cancellation. Figure 3-34 is a set of data presented as common offset data. The offset between geophone and shot is 14 m (45 ft). Note that the acoustic wave (visible as an arrival near 40 ms) is attenuated (the shot was buried for this record). Note the prominent reflection near 225 ms that splits into two arrivals near line distance 610 m. Such qualitative changes are the usual interpretative result of a common offset survey. No depth scale is furnished.

*c. Field techniques.* A shallow seismic reflection crew consists of three to five persons. The equipment used allows two to three times the number of active receivers to be distributed along the line. A switch (called a roll-along switch) allows the seismograph operator to select the particular set of geophones required for a particular shot from a much larger set of geophones that have been previously laid out. The operator can then switch the active array down the line as the position of the shot progresses. Often the time for a repeat cycle of the source and the archiving time of the seismograph are the determining factors in the production rates. With enough equipment, one or two persons can be continually moving equipment forward on the line while a shooter and an observer are sequencing through the available equipment.

(1) If the requirements for relative and absolute surveying are taken care of at a separate time, excellent production rates, in terms of number of shotpoints per day, can be achieved. Rates of 1/min or 400-500/normal field day can be achieved. Note that the spacing of these shot points may be only 0.6 to 1.2 m, so the linear progress may be only about 300 m of line for very shallow surveys. Also note that the amount of data acquired is

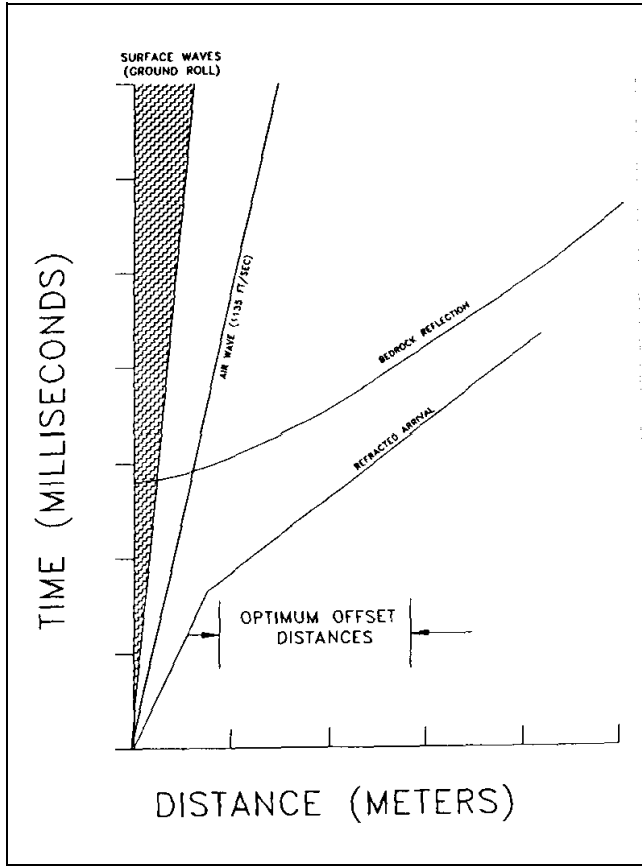


Figure 3-32. Optimum offset distance determination for the common-offset method

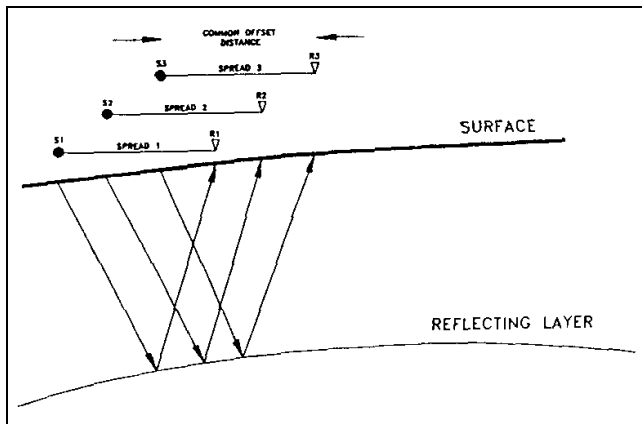


Figure 3-33. Common-offset method schematic

enormous. A 24-channel record sampled every 1/8 ms that is 200 ms long consists of nearly 60,000 thirty-two-bit numbers or upwards of 240 KB/record. Three hundred records may represent more than 75 MB of data for 1 day of shooting.

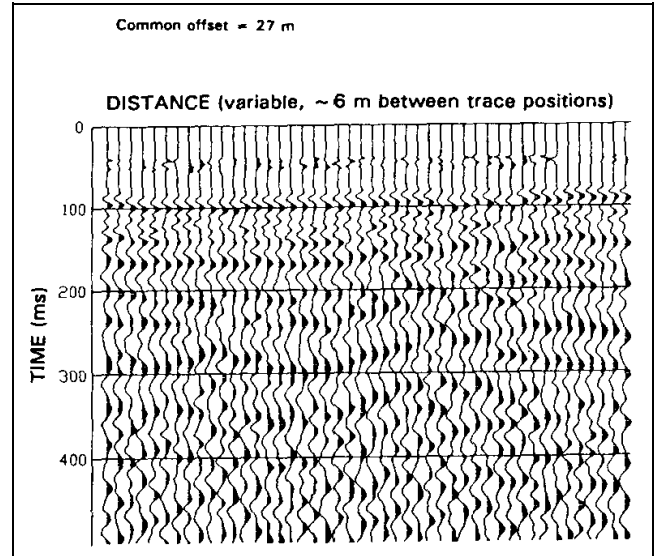


Figure 3-34. Sample common-offset record

(2) Field data acquisition parameters are highly site specific. Up to a full day of testing with a knowledgeable consultant experienced in shallow seismic work may be required. The objective of these tests is identifiable, demonstrable reflections on the raw records. If arrivals consistent with reflections from the zone of interest cannot be seen, the chances that processing will recover useful data are slim.

(3) One useful testing technique is the walkaway noise test. A closely spaced set of receivers is set out with a geophone interval equal to 1 or 2 percent of the depth of interest - often as little as 30 or 60 cm for engineering applications. By firing shots at different distances from this spread, a well-sampled long-offset spread can be generated. Variables can include geophone arrays, shot patterns, high and low-cut filters, and AGC windows, among others.

(4) Because one objective is to preserve frequency content, Table 3-2 is offered as a comparison between petroleum-oriented and engineering-oriented data acquisition. The remarks column indicates the reason for the differences.

*d. Processing.* Processing is typically done by professionals using special purpose computers. These techniques are expensive but technically robust and excellent results can be achieved. Exposition of all the processing variables is well beyond the scope of this manual. However a close association of the geophysicist, the processor,

**Table 3-2**  
**Seismic Reflection Use Differences by Methodology**

	Petroleum	Engineering	Remarks
Explosive seismic source	10-25 kg or more in a distributed pattern in deep holes	20 to 50 g, single shot	To increase frequency content
Mechanical seismic source	1-7 vibrators 5-15,000 kg peak force 10-100 Hz sweep	Hammer and Plats, guns <sup>1</sup>	Cost, increased frequency
Geophones	Arrays of 12-48 phones; 25-40 Hz fundamental frequency; 3-20 m spacing	Single or 3-5 geophones 50-100 Hz fundamental frequency; 1-3 m spacing	To preserve frequency content
Recorders	Instantaneous floating point, 48-1,000 channels	Instantaneous floating point, 24-96 channels	Cost
Passband analog filters	10-110 Hz	100-500 Hz	To increase frequency content
Sample interval	1-2 ms	1/4-1/8 ms	Higher frequencies

<sup>1</sup> High-frequency vibrators are becoming available in 1994.

and the consumer is absolutely essential if the results are to be useful. Well logs, known depths, results from ancillary methods, and the expected results should be furnished to the processor. At least one iteration of the results should be used to ensure that the final outcome is successful.

(1) One important conclusion of the processing is a true depth section. The production of depth sections requires conversion of the times of the reflections to depths by derivation of a velocity profile. Well logs and check shots are often necessary to confirm the accuracy of this conversion.

(2) These warnings are important because powerful processing algorithms can produce very appealing but erroneous results. Most data processors are oriented to petroleum exploration and volume production. The effort and cooperation required by both the geophysicist and the processor are beyond that normal in exploration scenarios.

*e. General conclusions-seismic reflection.*

(1) It is possible to obtain seismic reflections from very shallow depths, perhaps as shallow as 3 to 5 m.

(2) Variations in field techniques are required depending on depth.

(3) Containment of the air-blast is essential in shallow reflection work.

(4) Success is greatly increased if shots and phones are near or in the saturated zone.

(5) Severe low-cut filters and arrays of a small number (1-5) of geophones are required.

(6) Generally, reflections should be visible on the field records after all recording parameters are optimized.

(7) Data processing should be guided by the appearance of the field records and extreme care should be used not to stack refractions or other unwanted artifacts as reflections.

### 3-4. Surface Wave Methods

*a. Rayleigh wave methods.* A wide variety of seismic waves propagate along the surface of the earth. They are called surface waves because their amplitude decreases exponentially with increasing depth. The Rayleigh wave is important in engineering studies because of its simplicity and because of the close relationship of its velocity to the shear-wave velocity for earth materials. As most earth materials have Poisson's ratios in the range of 0.25 to 0.48, the approximation of Rayleigh wave velocities as shear-wave velocities causes less than a 10-percent error.

(1) Rayleigh wave studies for engineering purposes have most often been made in the past by direct observation of the Rayleigh wave velocities. One method consists of excitation of a monochromatic wave train and the direct observation of the travel time of this wave train between two points. As the frequency is known, the wavelength is determined by dividing the velocity by the frequency.

(2) The assumption that the depth of investigation is equal to one-half of the wavelength can be used to generate a velocity profile with depth. This last assumption is somewhat supported by surface wave theory, but more modern and comprehensive methods are available for inversion of Rayleigh-wave observations. Similar data can be obtained from impulsive sources if the recording is made at sufficient distance such that the surface wave-train has separated into its separate frequency components.

*b. Spectral analysis of surface waves (SASW).* The promise, both theoretical and observational, of surface wave methods has resulted in significant applications of technology to their exploitation. The problem is twofold:

(1) To determine, as a function of frequency, the velocity of surface waves traveling along the surface (this curve, often presented as wavelength versus phase velocity, is called a dispersion curve).

(2) From the dispersion curve, determine an earth structure that would exhibit such dispersion. This inversion, which is ordinarily done by forward modeling, has been automated with varying degrees of success.

*c. Measurement of phase velocity.* Spectral analysis, via the Fourier transform, can break down any time-domain function into its constituent frequencies. Cross-spectral analysis yields two valuable outputs from the simultaneous spectral analysis of two time functions. One output is the phase difference between the two time functions as a function of frequency. This phase difference spectrum can be converted to a time difference (as a function of frequency) by use of the relationship:

$$\Delta t(f) = \Phi(f)/2\pi f$$

where

$\Delta t(f)$  = frequency-dependent time difference

$\Phi(f)$  = cross-spectral phase at frequency  $f$

$f$  = frequency to which the time difference applies

(1) If the two time functions analyzed are the seismic signals recorded at two geophones a distance  $d$  apart, then the velocity, as a function of frequency, is given by:

$$V(f) = d/t(f)$$

where

$d$  = distance between geophones

$t(f)$  = term determined from the cross-spectral phase

If the wavelength ( $\lambda$ ) is required, it is given by

$$\lambda(f) = V(f)/f$$

(2) As these mathematical operations are carried out for a variety of frequencies, an extensive dispersion curve is generated. The second output of the cross-spectral analysis that is useful in this work is the coherence function. This output measures the similarity of the two inputs as a function of frequency. Normalized to lie between 0 and 1, a coherency of greater than 0.9 is often required for effective phase difference estimates.

(a) Once the dispersion curve is in hand, the calculation-intensive inversion process can proceed. While the assumption given above of depth equal to one half the wavelength may be adequate if relatively few data are available, the direct calculation of a sample dispersion curve from a layered model is necessary to account for the abundance of data that can be recorded by a modern seismic system. Whether or not the inversion is automated, the requirements for a good geophysical inversion should be followed and more observations than parameters should be selected.

(b) Calculation methods for the inversion are beyond the scope of this manual. The model used is a set of flat-lying layers made up of thicknesses and shear-wave velocities. More layers are typically used than are suspected to be present and one useful iteration is to consolidate the model layers into a geologically consistent model and repeat the inversion for the velocities only.

(3) The advantages of this method are:

(a) High frequencies (1-300 Hz) can be used, resulting in definition of very thin layers.

(b) The refraction requirement of increasing velocities with depth is not present; thus, velocities which decrease with depth are detectable.

By using both of these advantages, this method has been used to investigate pavement substrate strength. An example of typical data obtained by an SASW experiment is shown in Figure 3-35. The scatter of these data is smaller than typical SASW data. Models obtained by two different inversion schemes are shown in Figure 3-36



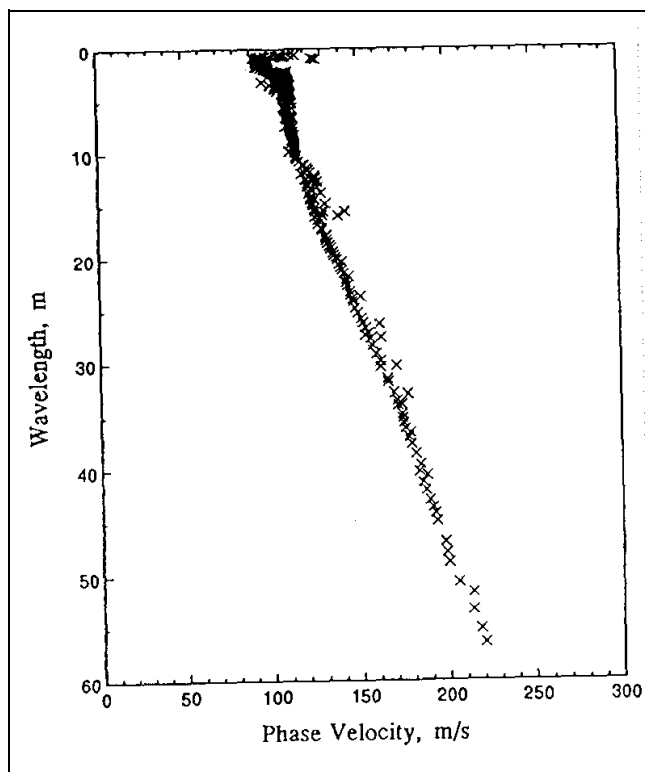


Figure 3-35. Typical SASW data

along with some crosshole data for comparison. Note that the agreement is excellent above 20 m of depth.

*d. Field work.* To date (1994) no commercial SASW equipment has been offered for sale. Most crews are equipped with a two- or four-channel spectrum analyzer, which provides the cross-spectral phase and coherence information. The degree of automation of the subsequent processing varies widely from laborious manual entry of the phase velocities into an analysis program to automated acquisition and preliminary processing. The inversion process similarly can be based on forward modeling with lots of human interaction or true inversion by computer after some manual smoothing.

(1) A typical SASW crew consists of two persons, one to operate and coordinate the source and one to monitor the quality of the results. Typical field procedures are to place two (or four) geophones or accelerometers close together and to turn on the source. The source may be any mechanical source of high-frequency energy; moving bulldozers, dirt whackers, hammer blows, and vibrators have been used. Some discretion is advised as the source must operate for long periods of time and the physics of what is happening are important. Rayleigh waves have

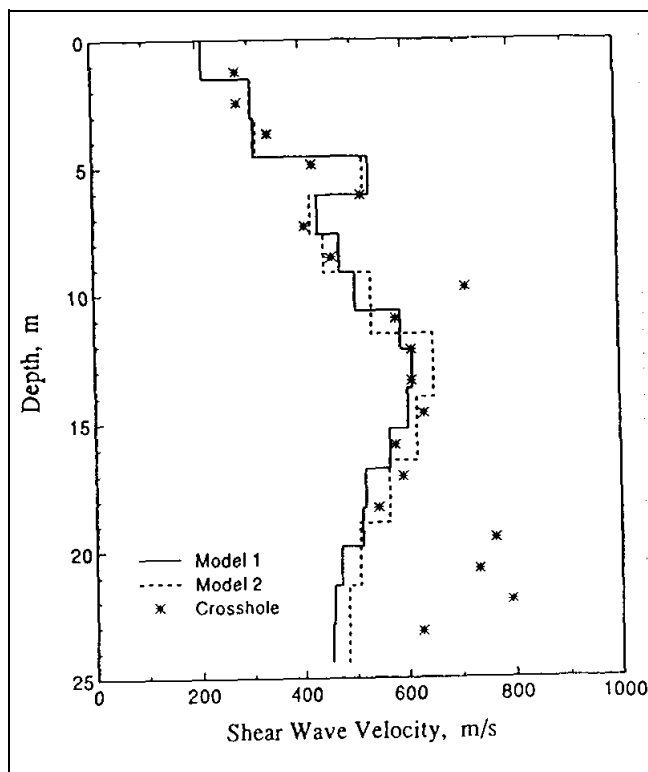


Figure 3-36. Inversion results of typical SASW data

predominantly vertical motion; thus, a source whose impedance is matched to the soil and whose energy is concentrated in the direction and frequency band of interest will be more successful.

(2) Phase velocities are determined for waves with wavelength from 0.5 to 3 times the distance between the geophones. Then the phones are moved apart, usually increasing the separation by a factor of two. Thus, overlapping data are acquired and the validity of the process is checked. This process continues until the wavelength being measured is equal to the required depth of investigation. Then the apparatus is moved to the next station where a sounding is required. After processing, a vertical profile of the shear-wave velocities is produced.

*e. Pitfalls.*

(1) The assumption of plane layers from the source to the recording point may not be accurate.

(2) Higher modes of the Rayleigh wave may be recorded. The usual processing assumption is that the fundamental mode has been measured.

(3) Spreading the geophones across a lateral inhomogeneity will produce complications beyond the scope of the method.

(4) Very high frequencies may be difficult to generate and record.

### 3-5. Subbottom Profiling

A variant of seismic reflection used at the surface of water bodies is subbottom profiling or imaging. The advantage of this technique is the ability to tow the seismic source on a "sled" or catamaran and to tow the line of hydrophones. This procedure makes rapid, continuous reflection soundings of the units below the bottom of the water body, in other words, the "subbottom." This method and significant processing requirements have been recently developed by Ballard et al. (1993) of the U.S. Army Engineer Waterways Experiment Station (WES). The equipment, acquisition, and processing system reduce the need for overwater boring programs. The developed WES imaging procedure resolves "material type, density, and thickness" (Ballard et al. 1993).

*a. Theory and use.* The acoustic impedance method may be exploited with other forms of Equations 3-2 and 3-14 to determine parameters of the soft aqueous materials. The acoustic impedance  $z$  for a unit is the product of its  $p_b$  and  $V_p$ . The reflection coefficient  $R$  from a particular horizon is

$$R = (E_{refl}/E_{inc})^{1/2} = [(z_i - z_j)/(z_i + z_j)] \quad (3-15)$$

where

$E_{refl}$  = energy reflected at the i-j unit boundary

$E_{inc}$  = incident energy at the i-j unit boundary

$z_i$  = acoustic impedance of the i (lower) material

$z_j$  = acoustic impedance of the j (upper) medium

At the highest boundary, the water-bottom interface,  $z_{j,water}$  is known to be  $1.5 \times 10^9$  g/(m<sup>2</sup>s). Since the  $E_{refl,1-2}$  can be determined and  $E_{inc,1-2}$  and  $z_{1,water}$  are known,  $z_{i,2}$  may be determined.  $V_{p,2}$  may be assessed from the depth of the 2-3 boundary and thus  $\rho_{i,2}$  may be resolved. The material properties of lower units can be found in succession from the reflections of deeper layers.

(1) A variety of different strength sources are available for waterborne use. By increasing strength, these

sources are: pingers, boomers, sparkers, and airguns. While there is some strength overlap among these sources, in general, as energy increases, the wave's dominant period increases. For the larger source strength, therefore, the ability to resolve detail is impaired as period and wavelength become larger. The resolving accuracy of the system may change by more than an order of magnitude from <0.2 m for a pinger to >1.0 m for an airgun.

(a) The WES Subbottoming System has two sources: a 3.5- and 7.0-kHz pinger and a 0.5- to 2.5-kHz broad spectrum boomer. The pinger can attain resolutions to 0.2 m, while the boomer has a resolution on the order of 1/2 m.

(b) The conflicting impact of energy sources is the energy available for penetration and deeper reflections. The boomer's greater energy content and broad spectrum allow significantly greater depth returns. Some near-bottom sediments contain organic material that readily absorbs energy. Higher energy sources may allow penetration of these materials.

(2) Data collection is enormous with a towed subbottoming system. Graphic displays print real-time reflector returns to the hydrophone set. Recording systems retrieve the data for later processing. The field recorders graph time of source firing versus time of arrival returns. Figure 3-37 provides the field print for Oakland Harbor (Ballard, McGee, and Whalin 1992).

(a) Office processing of the field data determines the subbottoming properties empirically. The empiricisms are reduced when more sampling (boring) data are available to assess unit  $\rho$  and loss parameters for modeling. The processing imposes the Global Positioning System (GPS) locations upon the time of firing records to approximately locate the individual "shot" along the towed boat path. The seismic evaluation resolves the layer  $V_p$  and unit depths. From the firing surface locations and unit depths, the field graphs are correlated to tow path distance versus reflector depths. Figure 3-38 shows cross sections of the Gulfport Ship Channel, Mississippi. These are fence diagrams of depth and material types once all parallel and crossing surveys are resolved.

(b) WES processing capabilities now allow 3-dimensional surfaces to be mathematically appraised from the fence diagrams. These computer volumetric depictions are convenient for visualizing the subsurface deposition. More importantly, direct volume estimates and project development can be created.

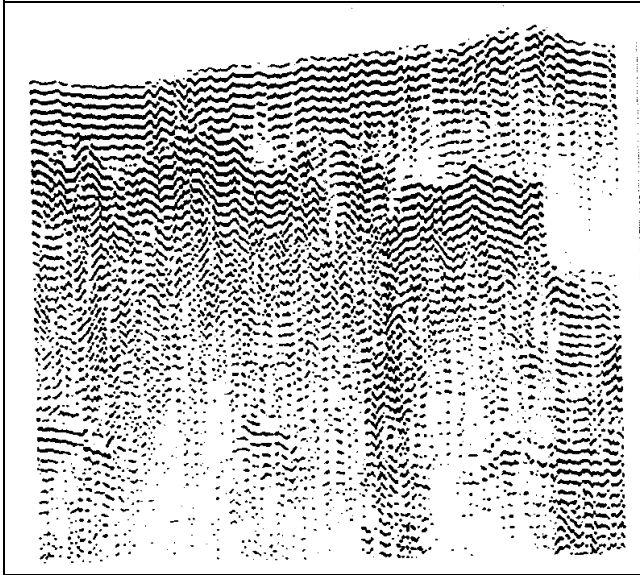


Figure 3-37. Reflected subbottoming signal amplitude cross section-3.5 kHz in Oakland Harbor, California (Ballard, McGee, and Whalin 1992)

*b. Availability.* Research at the U.S. Army Engineer Waterways Experiment Station (WES) has developed oil exploration techniques for engineering projects.

(1) The original research interest was dredging material properties. The current system has been combined with GPS to locate the continuous ship positions for knowing the source/hydrophone locations.

(2) WES has a Subbottom Imaging System to provide data for engineering projects in coastal, river and lake environments. The WES Subbottoming System is ship-mounted, so that it can be shipped overland to differing marine environments.

(3) The subbottoming technique can be applied to a large variety of water bodies. Saltwater harbors and shipping channels and river waterways were the original objective for the dredging research. The developed system has broad applicability to locks and dams, reservoir projects, and engineering projects such as location of pipelines.

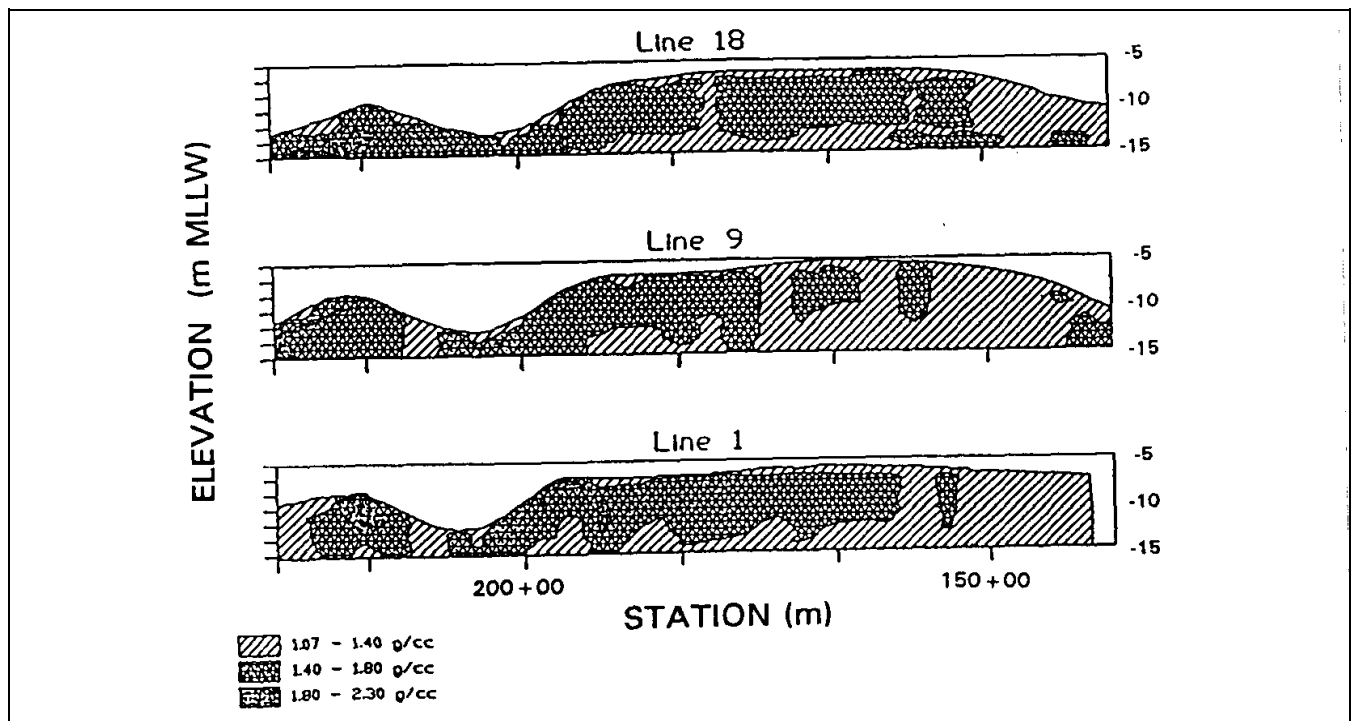


Figure 3-38. Density cross sections in Gulfport Ship Channel, Mississippi (Ballard, McGee, and Whalin 1992)